STRESS DISTRIBUTION IN PIPE ELLS WITH STRAIGHT END EXTENSIONS UNDER INTERNAL PRESSURE

WILLIAM HENDERSON PRICE, Jr.

and

JOHN WHITFIELD McADAMS, Jr.

STRESS DISTRIBUTION IN PIPE ELLS WITH STRAIGHT END EXTENSIONS UNDER INTERNAL PRESSURE

* * * * * * *

William Henderson Price, Jr.

and

John Whitfield McAdams, Jr.

STRESS DISTRIBUTION IN PIPE ELLS WITH STRAIGHT END EXTENSIONS UNDER INTERNAL PRESSURE

by

William Henderson Price, Jr.,
Lieutenant Commander, United States Navy

and

John Whitfield McAdams, Jr.,
Lieutenant, United States Navy

Submitted in partial fulfillment
of the requirements
of
MASTER OF SCIENCE
IN
MECHANICAL ENGINEERING

United States Naval Postgraduate School
Monterey, California

1954

This work is accepted as fulfilling
the thesis requirements for the degree of

MASTER OF SCIENCE
IN
MECHANICAL ENGINEERING

from the

United States Naval Postgraduate School.

PREFACE

The experimental investigation of stresses in steel pipe ells under internal static pressure, herein reported, was conducted at the U. S. Naval Postgraduate School from January to April 1954. Professor R. E. Newton acted as faculty advisor.

The three specimens tested were selected from a group of five made available by the Midwest Piping Co., Inc., St. Louis, Missouri, through the courtesy of Doctor John E. Brock, Research Director.

R. J. Le Ber and J. W. Morrison [6]≠ in 1953 completed a series of similar experiments utilizing the five specimens and recommended further experimentation which they lacked time to complete.

The purpose of additional investigation was to verify and if possible to amplify the results obtained by Le Ber and Morrison utilizing higher pressures and some variations in technique.

The authors take this opportunity to express their gratitude to Professor Newton for his very valuable assistance and guidance in all phases of the work undertaken and to Doctor Brock for his assistance in making available the pipe specimens as well as helpful literature pertinent to the project.

≠ Numbers in brackets refer to items in bibliography.

TABLE OF CONTENTS

LIST OF ILLUSTRATIONS

SYMBOLS AND ABBREVIATIONS

d	Diameter of pipe cross section	inches
E	Young's modulus of elasticity = 29.6×10^6	psi
P	Internal static gage pressure	psi
R	Mean radius of pipe ell to center line of pipe	inches
r	Radius of pipe cross section	inches
t	Wall thickness of pipe	inches
e	Measured apparent strain on external surface	microinches/inch
$\bar{e}$	Measured apparent strain on internal surface uncorrected for pressure effects on compensating gage mounting block	microinches/inch
ϵ	Actual experimental strain	microinches/inch
$\bar{\epsilon}$	Measured strain on internal surface corrected for transverse sensitivity but uncorrected for pressure effects on compensating gage mounting block	microinches/inch
ν	Poisson's ratio = 0.3	
σ	Normal stress	psi
k	Transverse sensitivity factor for SR-4 strain gages	
ϕ	Angle between t direction and maximum principal stress direction	degrees

SUBSCRIPTS

i	Internal surface of pipe
o	External surface of pipe
t	Tangential or hoop direction
l	Longitudinal or meridional direction
m	Arithmetic mean between internal and external values
b	45 degree direction midway between l and t directions.

CHAPTER I

OBJECTIVE AND SUMMARY

The primary objective of this project was to determine experimentally the stress distribution at selected locations in thick wall 90° steel pipe ells, with straight end extensions, under internal hydrostatic pressure. Secondary objectives were to gain knowledge of the technique of using SR-4 strain gages subjected to pressure and to explore more fully the area in the specimens near the point of maximum stress (reported by Le Ber and Morrison to be at the quarter point of the 90° bend).

A comparison of the results obtained is made with available theory as well as with results reported by Le Ber and Morrison≠ on the same specimens in 1953.

Specimens tested were those numbered 1, 2, and 4 by Le Ber and Morrison having wall thicknesses of 0.32, 0.50, and 0.50 inches and mean bend radii of 12, 12, and 8 inches, respectively.

SR-4 strain gages were placed at selected internal and external locations (Figs. 1, 2, and 3). Oil was used as the pressure medium. Of particular interest was the stress distribution at the transition section where the geometrical configuration does not approximate either the straight pipe conditions of G. Lamé's [8] theory nor the torus condition assumed in the theories of W. R. Dean [3] and A. Föppl [4].

Tangential and longitudinal stresses were computed from developed strain data using Hooke's law and standard reduction formulas for SR-4 strain gages.

≠ Hereafter referred to as L and M

The maximum stress in each specimen was found to be on the internal surface along the 0° meridian (inside the bend) in the tangential direction as predicted by the theories of Föppl and Dean. In the three specimens tested the maximum stress occurred at the $22\ 1/2^{\circ}$ or quarter point at the bend as reported by L and M. However, in each of the three specimens no great variation in the stress between the $22\ 1/2^{\circ}$ and the 0° or mid-point of the 90° bend was found.

The maximum stress in the specimens was found to be from 16% to 39% greater than that calculated by Dean's formula and from 4% lower to 25% greater than that calculated by Föppl's formula.

Within the accuracy of experimentation the principal stress directions at the transition section were found to substantially coincide with the longitudinal and tangential directions.

In general strain gages on the external surfaces were more reliable than those on internal surfaces. Much better results were obtained internally with single element type A-5 gages than with the AX-5 type. Extreme care in surface preparation and gage installation technique was found to be required for internal gages.

CHAPTER II

SPECIMEN DESCRIPTION AND PREPARATION

1. General Description

The specimens used in this investigation were three of a group of five pipe ells used by L and M in 1953. Their paper gives a complete description of these ells, and only a brief resume will be given here. The specimens consisted of nominal 8 inch seamless steel butt welding elbows with straight lengths of pipe welded thereto. They were furnace stress relief annealed after welding and the welds were ground down, inside and outside, to somewhat better than commercial standards. The specimens tested were:

Number (L and M)	Bend radius	Wall thickness
1	12 in.	0.32 in.
2	12 in.	0.50 in.
4	8 in.	0.50 in.

These three were chosen to give a variation in both the parameters of wall thickness and bend radius.

2. Preparation for Testing

The first specimen studied was No. 4. All inside gages were removed and the surfaces were ground moderately well with a grinding wheel mounted on a small electric drill followed by hand polishing with emery cloth. This left the surface with far from the optimum smoothness but was considered the best that could be done in the time available. There were several deep pits in the weld metal at the transition section which were not ground out. Surfaces where gages were to be applied were cleaned with toluene and acetone before cement was applied. The

gages were mounted by placing them in position relative to each other on a piece of masking tape and then inserting the tape in the pipe to previously measured locations. The gage leads had to be soldered to the gages prior to insertion. This tended to make the tape unwieldy but no better method could be devised at the time. All inside X-type gages used were type AX-5. Single element gages of type A-5 were installed at the transition section in the longitudinal, tangential, and b directions.

On the outside, the old gages were used with gages added at the $11\ 1/4^{\circ}$ and $33\ 3/4^{\circ}$ points on the 0° meridian and defective gages replaced. The outside surfaces were prepared for gage installation using standard techniques. Figure 1 is a sketch of Specimen 4 showing pertinent dimensions and gage locations.

The second specimen considered was No. 2. Here all inside AR-1 gages and only the AX-5 gages which the previous work indicated as doubtful or defective were replaced. Additional gages were added along the 0° meridian. The proximity of other gages and their lead wires made it necessary to restrict the preparation of the surface to dressing with emery cloth. Again this left the surface in rather poor condition. The gages which were replaced on the inside were applied with essentially the same cleaning and cementing techniques as in the first specimen tested. Figure 2 is a sketch of Specimen 2 with gage locations and pertinent dimensions.

The third and last specimen tested was No. 1. In view of the results obtained with the previous specimens, it was felt that more emphasis should be given to preparation of the surfaces upon which the gages were mounted. Another refinement which seemed to be

indicated was the exclusive use of single element gages inside. Accordingly, all old interior gages were removed and the surfaces given extensive preparation. They were ground fairly smooth with the grinding wheel and electric drill mentioned above and then polished with emery cloth mounted on a carpenter's sanding drum. Approximately thirty hours were spent in this preparation and a fairly good surface resulted. A few of the gage locations in the transition section still had deep pits in the weld metal, and these were removed insofar as possible.

A rather novel method of gage locating was devised for this specimen. Since, in using single element gages, as many gages as possible are required in order to obtain adequate data, a total of 45 type A-5 gages were installed. This was the maximum number of leads available through the transfer block. To position these gages accurately, with their wires soldered in place, was a difficult problem. The solution adopted required the construction of a "cage" from 2 1/2 inch strips of manila paper, cut and fitted so that it conformed to the inner surface of the specimen. Before assembly, rectangular holes were cut in these strips at the desired gage locations which were slightly larger than the backing paper of type A-5 gages. Orthogonal lines were also drawn on the strips for matching with the lines on the gage backing paper. This paper cage was then assembled, placed in the pipe, and secured. The gages were installed individually in the holes mentioned. This facilitated gage installation, especially when the location could be seen only by looking into a mirror. The interior of the pipe was heated with electric light bulbs for 48 hours to aid in drying the cement completely before filling with oil.

The exterior gages which were applied were handled in the normal routine manner, as before. Figure 3 is a sketch of Specimen 1 showing pertinent dimensions and gage locations.

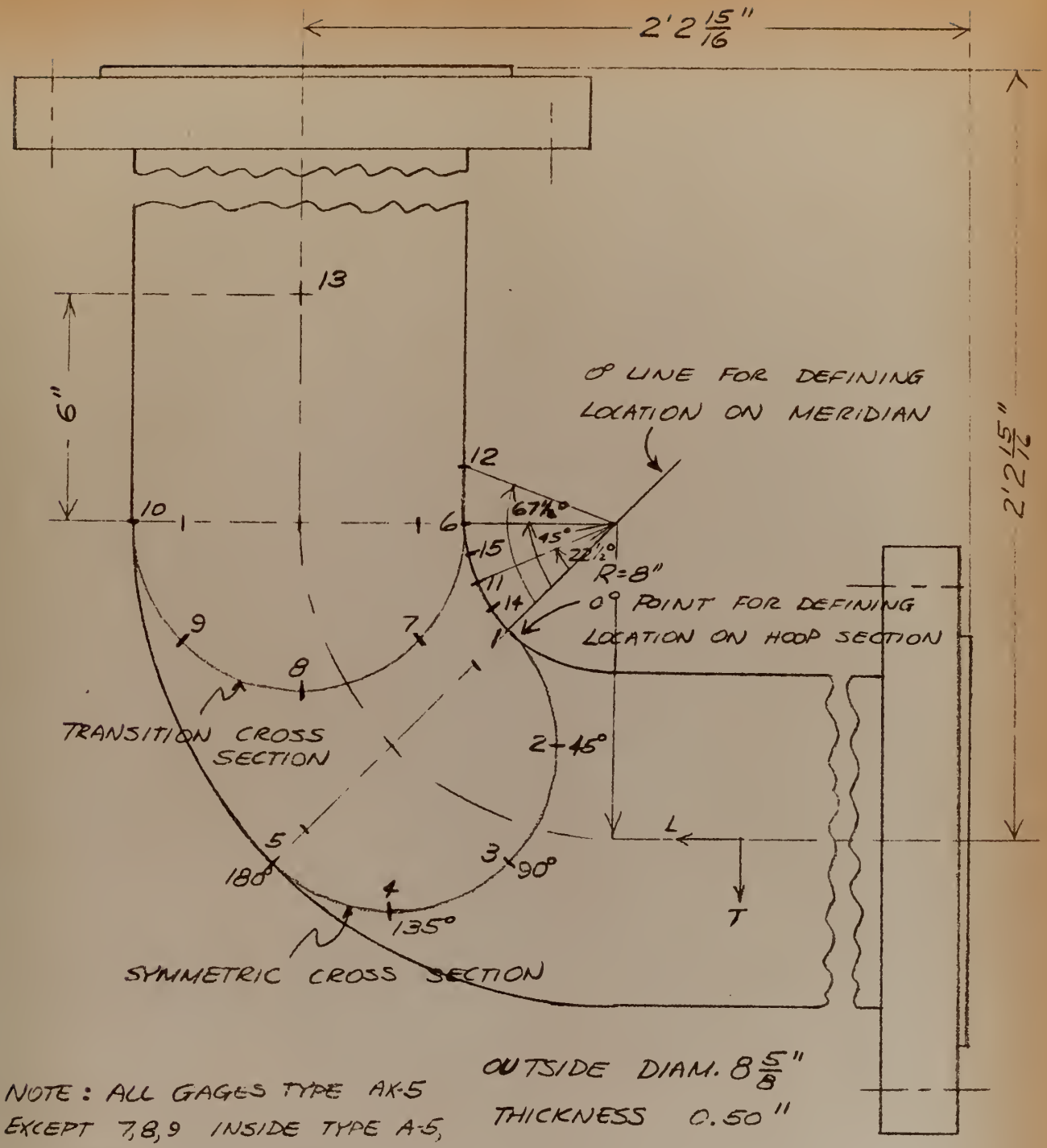

NOTE: ALL GAGES TYPE AX-5 EXCEPT 7,8,9 INSIDE TYPE A-5, OUTSIDE TYPE AR-1.

FIG. 1

SPECIMEN NO.4 - DIMENSIONS & GAGE LOCATIONS

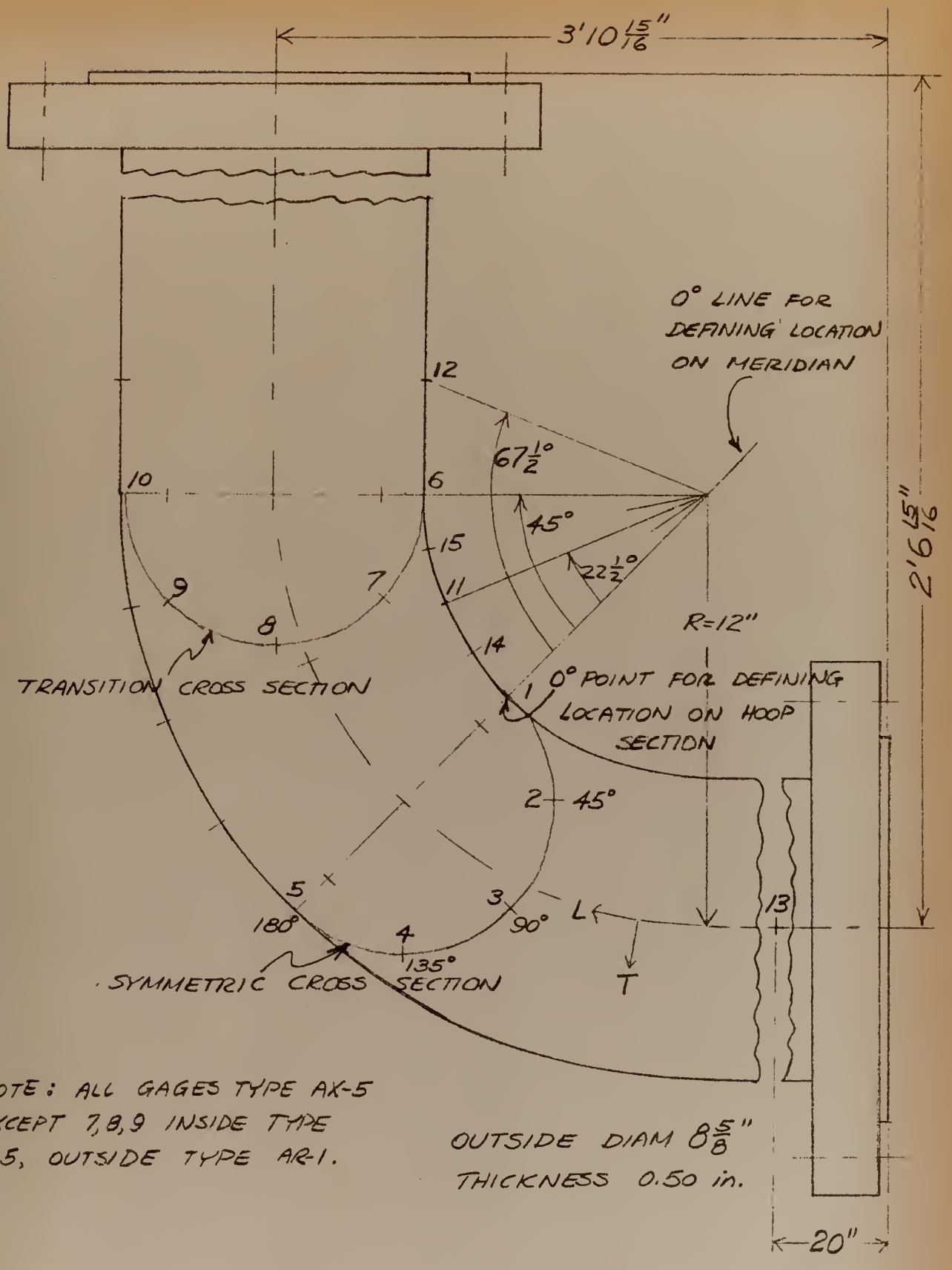

FIG. 2

SPECIMEN NO. 2 - DIMENSIONS & GAGE LOCATIONS

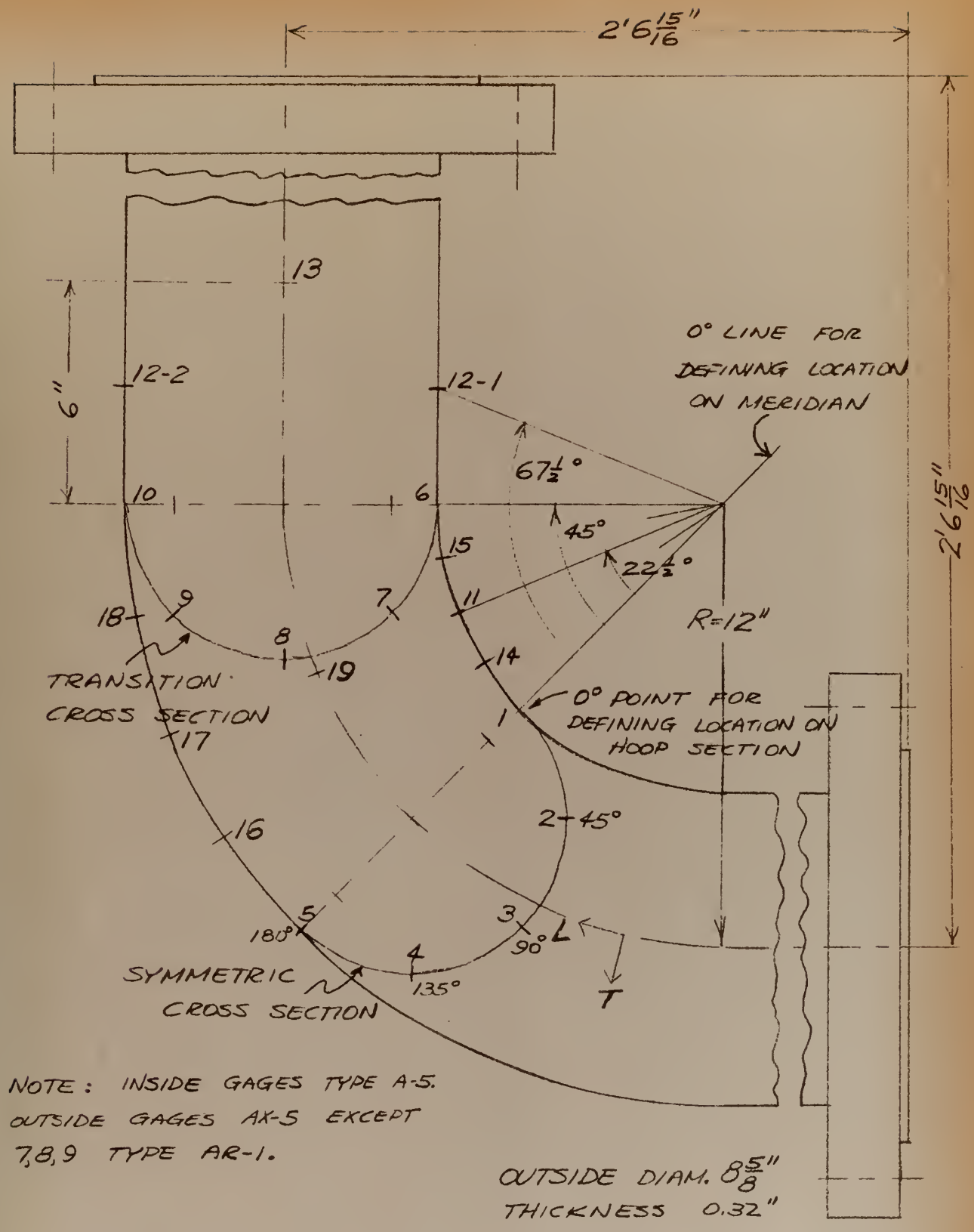

FIG. 3

SPECIMEN NO. 1 - DIMENSIONS & GAGE LOCATIONS

CHAPTER III

EXPERIMENTAL TECHNIQUE

The lead wires for the inside gages were of No. 22 AWG solid copper enameled wire. This wire was chosen as a compromise between the flexibility and the cross-sectional area desired. A larger wire area would have been better from the viewpoint of lead resistance but the need for soldering wires on gages before insertion made flexibility an important consideration also. The wires were all cut to the same length to minimize bridge unbalance due to the effects of pressure on the lead wires.

These inside gage wires were brought out of the pipe through a specially designed pressure fitting. Figure 4 is a drawing of this fitting showing in detail its construction. The enameled wires were first soldered to terminal strips. From these terminals, No. 22 AWG solid copper thermoplastic insulated wires were led through the pressure fitting to the exterior of the pipe and eventually to the measuring apparatus. Small tapered bushings of lucite were slipped over the individual wires and then driven into tapered holes in the brass plate. Even with this tapered plug in tapered hole arrangement, a few small leaks were noted. These were not serious enough to limit the maximum pressure attainable.

The end flanges were secured to the pipe using twelve, one inch, high tensile steel studs. This steel was of 100,000 psi minimum ultimate tensile strength. The gaskets were of 0.064 inch fully annealed

copper sheet. The studs were made up with a torque wrench to 300 foot pounds torque using a skip sequence. No appreciable leakage was noted on any of the specimens at the end flanges.

Hydrostatic pressure was obtained by the use of a Watson-Stillman hand pump with a light oil as the medium. The use of oil made waterproofing of the gages unnecessary.

Pressure measurement was by means of a piston type dead weight gage tester connected directly to the end flange on the specimen. The weights were kept floating by use of the pump, giving a fixed pressure. A 5000 psi Bourdon gage was also used as an approximate pressure indication. Specimens 2 and 4 were tested to 2000 psi and Specimen 1 to 1500 psi. Ascending and descending increments of 500 psi were used.

The pipe specimens were tested in the horizontal position. In order that the specimens be free to deform, the center of the ell and one end flange were supported individually on three one inch steel balls between flat steel plates. This removed any restraint which might lead to external horizontal forces on the pipe ell.

Before readings of strain were made, the specimens were exercised by pressure cycling from zero to the maximum to be used at least five times. Differential strain readings were then made using a Baldwin SR-4 Model K Strain Indicator. The active gage leads were led to SR-4 Switching and Balancing Units which were used simply as multi-position switches. The output of these switching units was connected to the Model K indicator. The leads from the compensating gage

were connected directly to the binding posts on the indicator. This was necessary since the resistors in the balancing unit were not subjected to the hydrostatic pressure and full compensation for pressure effects on the active gage could not otherwise be realized.

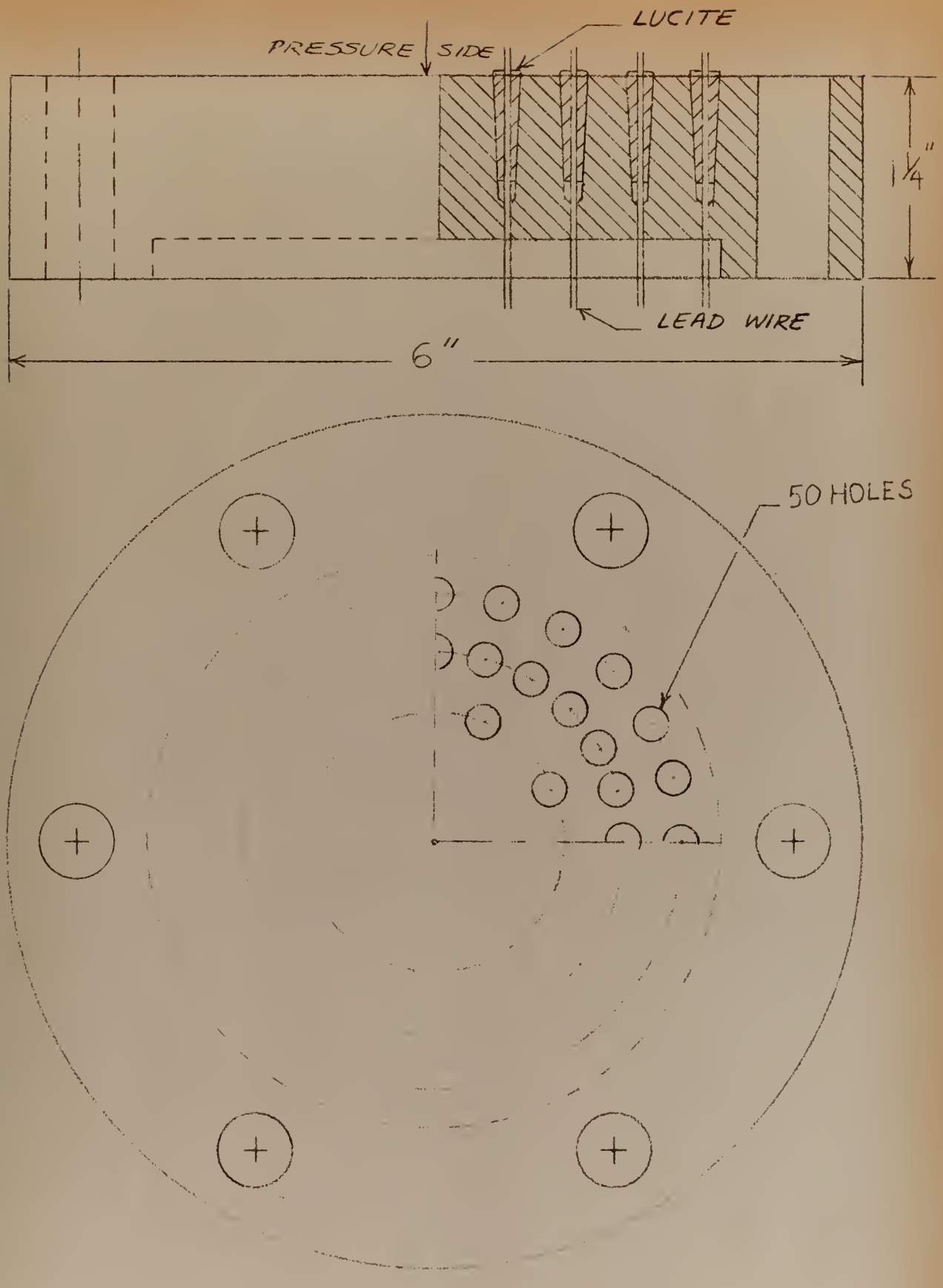

FIG. 4 - LEAD WIRE TRANSFER FITTING

CHAPTER IV

RESULTS AND RELIABILITY

1. Results

The experimental results obtained with the three specimens are shown in the accompanying graphs and tables. Curves of $\frac{\sigma_{\ell i}}{P}$, $\frac{\sigma_{\ell o}}{P}$, $\frac{\sigma_{ti}}{P}$, and $\frac{\sigma_{to}}{P}$ versus angular location are shown in Figures 5 through 9 for Specimen 1, Figures 10 through 12 for Specimen 2 and Figures 13 through 15 for Specimen 4.

In Figures 16 through 18 experimental values of $\frac{\sigma_{\ell m}}{P}$ and $\frac{\sigma_{tm}}{P}$ vs. angular location and corresponding theoretical values are plotted for Specimens 2 and 4 (equal wall thickness, varying bend radius). Figures 19 through 21 are similar curves for Specimens 1 and 2 (equal bend radii, varying wall thickness).

Tables I through III show, respectively: Tabular comparisons of the maximun $\frac{\text{stress}}{\text{pressure}}$ ratio found in each specimen with applicable theoretical values; comparison of $\frac{\sigma_t}{P}$ in the straight end extensions with Lamé's theory; and the principal stress directions obtained at transition sections. Experimental values of $\frac{\sigma}{P}$ at each gage location are given in Table IV and the measured apparent strains from which they were obtained in Table V.

Table I. Comparison of Maximum Experimental Values of σ/p with Theoretical Values

Specimen No.	$\frac{\sigma_{tm}}{p}$ - Dean	$\frac{\sigma_{tm}}{p}$ - Föppl	$\frac{\sigma_{tm}}{p}$ - Experimental	Meridian location of $\frac{\sigma_{tm}}{p}$ in ell	Cross section	$\frac{\sigma_{ti}}{p}$ - Experimental	Meridian location of $\frac{\sigma_{ti}}{p}$ in ell	Cross section
1	15.2	16.3	14.4	0°	0°	19.2	0°	22 1/2°
2	9.23	10.2	10.7*	0°	22 1/2°	12.8*	0°	22 1/2°
4	10.3	12.4	10.5	0°	22 1/2°	11.9	0°	22 1/2°

* Plot of inside apparent strain not a good straight line.

Table II. Comparison of $\frac{\sigma_t}{p}$ in Straight Pipe (gage location 13) with Lamé's Theory

Specimen No.	Wall thickness - inches	Bend radius - inches	Lamé		Experimental	
			$\frac{\sigma_{ti}}{p}$	$\frac{\sigma_{to}}{p}$	$\frac{\sigma_{ti}}{p}$	$\frac{\sigma_{to}}{p}$
1	.32	12	13.0	12.0	11.6	12.8
2	.50	12	8.17	7.15	9.10*	6.89
4	.50	8	8.17	7.15	7.65	6.86

* Plot of inside apparent strain not a good straight line.

Table III. Principal Stress Directions at Transition Sections with Respect to t Direction

Gage Location	Specimen No. 1		Specimen No. 2		Specimen No. 4	
	ϕ_i	ϕ_o	ϕ_i	ϕ_o	ϕ_i	ϕ_o
7	4°	2°	0°	0°	6°	2°
8	1°	4°	4°	6°	2°	2°
9	4°	3°	9°	0°	6°	2°

Table IV. Experimentally Determined Values of $\frac{\sigma}{p}$

Gage Location and direction	Specimen No. 1		Specimen No. 2		Specimen No. 4	
	$\frac{\sigma_i}{p}$	$\frac{\sigma_o}{p}$	$\frac{\sigma_i}{p}$	$\frac{\sigma_o}{p}$	$\frac{\sigma_i}{p}$	$\frac{\sigma_o}{p}$
1 l	7.70	5.32	7.30*	3.43	1.30*	3.02
1 t	17.7	11.1	10.9*	8.75	10.8*	9.32
2 l	5.92	2.95	2.40	4.01	1.76*	2.67
2 t	13.7	11.0	8.36	9.26	8.90*	7.59
3 l	5.40	7.10	5.65*	4.28	4.05	3.24
3 t	9.75	15.2	11.2*	6.95	7.36	6.25
4 l	6.56	7.10	4.88	3.30	3.90	2.69
4 t	10.8	10.3	9.07	6.02	7.40	4.67
5 l	4.94	3.79	3.76	3.74	7.34*	2.84
5 t	12.8	8.36	6.72	6.80	8.00*	5.54
6 l	7.74	5.55	4.69	4.17	5.14	3.23
6 t	16.0	10.8	10.7	8.36	10.6	8.34
7 l	5.74	4.99	3.29	3.96	3.34	2.96
7 t	12.8	11.7	9.40	8.18	8.60	7.16
8 l	4.70	5.71	3.45	4.10	4.31	3.45
8 t	10.3	13.1	8.66	6.94	8.25	7.01
9 l	5.73	6.24	3.39	4.33	4.62	3.32
9 t	12.7	11.8	8.35	7.22	8.69	6.32
10 l	5.76	4.36	4.03	3.16	2.38*	2.79
10 t	15.3	9.24	8.35	6.65	7.64*	6.23
11 l	8.26	3.78	4.19*	3.53	1.41	3.88
11 t	19.2	8.48	12.8*	8.60	11.9	9.16
12-1 l	6.78	4.96	5.87*	3.44	4.57	2.40
12-1 t	14.7	8.88	11.0*	6.86	9.50	6.03
12-2 l	6.53	5.09	- -	- -	- -	- -
12-2 t	15.9	10.1	- -	- -	- -	- -
13 l	5.40	6.16	5.40*	3.51	3.34	3.34
13 t	11.6	12.8	9.10*	6.89	7.65	6.86
14 l	8.34	4.44	7.70*	3.38	1.12	2.92
14 t	19.0	9.46	12.1*	8.11	10.4	9.18
15 l	7.55	3.51	8.40*	3.63	0.95*	4.27
15 t	18.1	8.67	12.1*	8.70	9.42*	9.52
16 l	5.29	3.76				
16 t	14.1	8.69				
17 l	5.33	3.97				
17 t	14.1	8.99				
18 l	5.10	4.79				
18 t	12.9	9.60				
19 l	6.26	- -				
19 t	8.54	- -				

* Plot of inside apparent strain not a good straight line.

Table V. Apparent Strain (microinches per inch per psi) Uncorrected for Transverse Sensitivity or Effect of Pressure on Inside Compensating Gage Mounting Block

Gage location and direction	Specimen No. 1		Specimen No. 2		Specimen No. 4	
	$\frac{\bar{e}_i}{p}$	$\frac{e_o}{p}$	$\frac{\bar{e}_i}{p}$	$\frac{e_o}{p}$	$\frac{\bar{e}_i}{p}$	$\frac{e_o}{p}$
1 l	.123	.078	.170*	.036	-.038*	.017
1 t	.550	.325	.325*	.262	.388*	.285
2 l	.100	.000	.027	.050	-.002*	.021
2 t	.430	.341	.292	.274	.307*	.230
3 l	.118	.101	.110*	.080	.090	.052
3 t	.202	.445	.350*	.194	.233	.180
4 l	.147	.145	.100	.056	.094	.048
4 t	.328	.280	.306	.171	.236	.132
5 l	.075	.052	.090	.065	.194*	.045
5 t	.410	.244	.216	.194	.223*	.160
6 l	.140	.088	.084	.064	.095	.033
6 t	.490	.313	.340	.243	.333	.250
7 l	.102	.059	.050	.056	.054	.032
7 b	.273	.194	.179	.146	.192	.129
7 t	.403	.345	.309	.237	.282	.213
8 l	.090	.067	.062	.073	.090	.050
8 b	.212	.248	.155	.146	.170	.131
8 t	.327	.389	.282	.194	.260	.203
9 l	.102	.109	.063	.078	.096	.052
9 b	.232	.195	.133	.141	.166	.111
9 t	.400	.305	.272	.202	.272	.181
10 l	.080	.063	.084	.046	.032*	.037
10 t	.485	.270	.267	.194	.258*	.183
11 l	.129	.050	.049*	.041	-.043	.047
11 t	.594	.250	.432*	.256	.412	.272
12 -1 l	.117	.086	.122*	.053	.087	.026
12 -1 t	.457	.253	.341*	.199	.299	.180
12 -2 l	.100	.074				
12 -2 t	.500	.293				
13 l	.100	.091	.122*	.055	.065	.050
13 t	.368	.373	.280*	.199	.248	.200
14 l	.136	.059	.174*	.036	-.038	.015
14 t	.575	.276	.360*	.240	.364	.281
15 l	.115	.035	.198*	.039	-.034*	.057
15 t	.562	.258	.355*	.257	.332*	.280
16 l	.075	.043				
16 t	.450	.256				
17 l	.076	.047				
17 t	.450	.264				
18 l	.080	.069				
18 t	.410	.277				
19 l	.158					
19 t	.254					

* Plot of inside apparent strain not a good straight line.

2. Reliability of Results

Values of σ/p calculated from experimental data are estimated to be in error by no more than 5% for all gage locations in the specimens with the exception of those internal locations indicated by an asterisk in Tables IV and V. For those latter locations the maximum error is roughly estimated to be between 15% and 20%.

Equilibrium checks were made where possible by graphical integration with the following percentage errors in the results.

Specimen No.	Location		
	Symmetric section in l direction	Transition section in l direction	0° and 180° meridians** in t direction
1	2%	4%	1/3 %
2	16% *	5%	-
4	10% *	1%	-

* Includes results of poor reliability as indicated in Table IV.

** A free body was taken bounded by the 0° and 180° meridian, the symmetric cross section and the cross section at gage point 13.

Comparison of results with theory from the viewpoint of possible indications of the degree of reliability in the experimental data is considered to be of little value. This opinion is based upon the fact that the geometrical configuration, including ovality at cross sections, is not that assumed by theory.

The somewhat erratic and unexpected maxima and minima in several of the σ/p versus location curves are believed to be due in part to indicated unreliable data but also to the influence of cross section ovality.

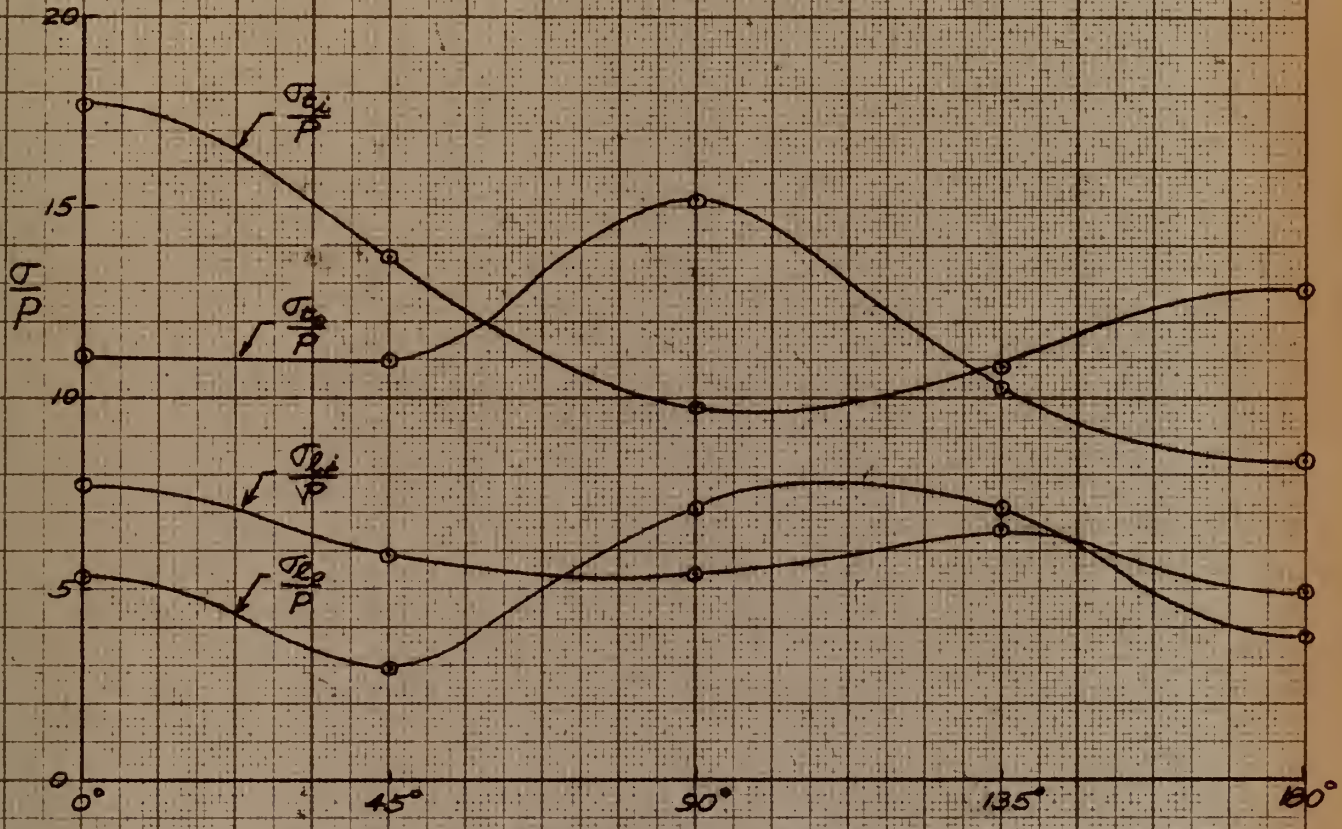

FIG. 5

SPECIMEN NO. 1

SYMMETRIC CROSS SECTION

STRESS/PRESSURE RATIO VS. ANGULAR LOCATION

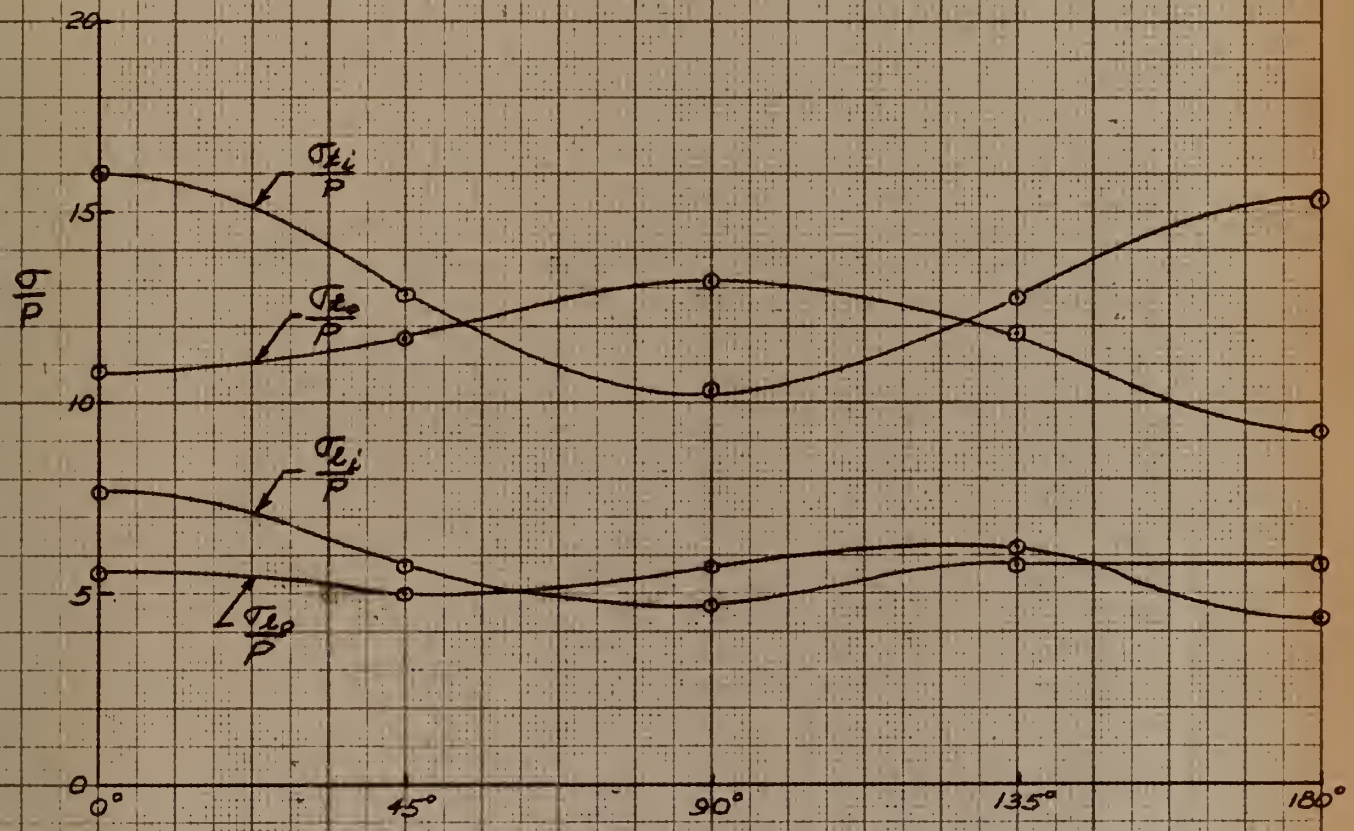

FIG. 6

SPECIMEN NO. 1

TRANSITION CROSS SECTION

STRESS/PRESSURE RATIO VS. ANGULAR LOCATION

FIG. 7

SPECIMEN NO. 1

0° MERIDIAN

STRESS/PRESSURE RATIO VS. ANGULAR LOCATION

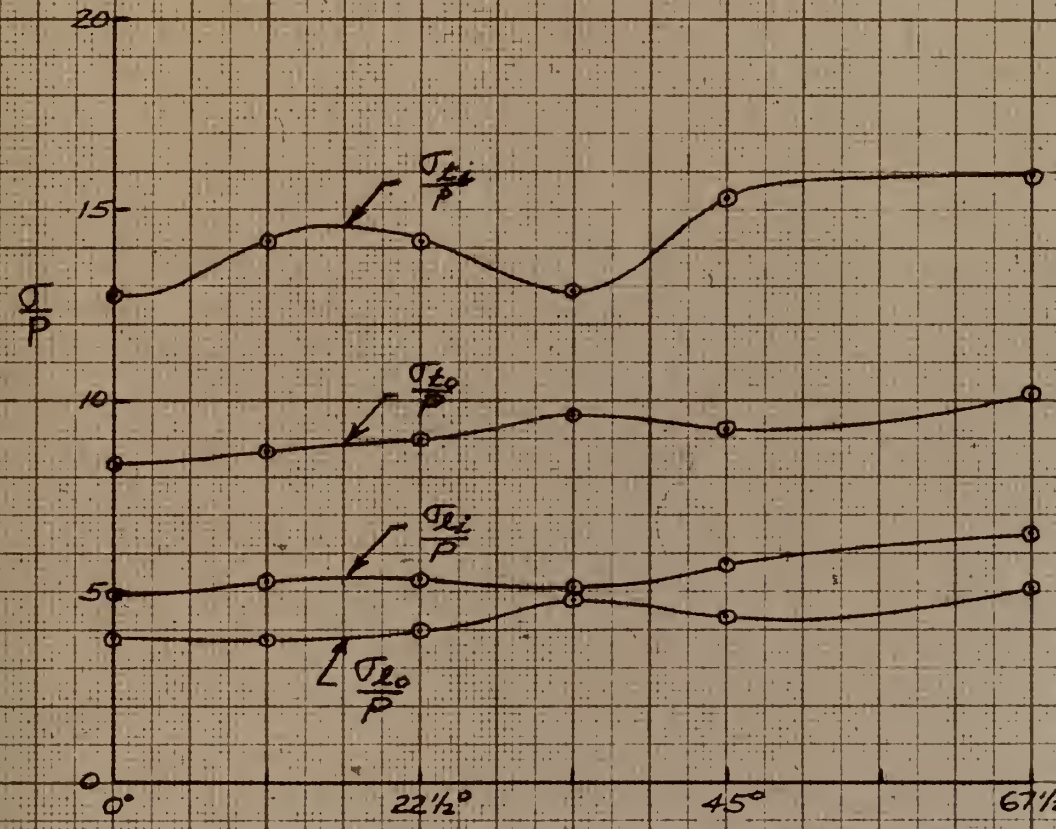

FIG. 8

SPECIMEN NO. 1

180° MERIDIAN

STRESS/PRESSURE RATIO VS. ANGULAR LOCATION

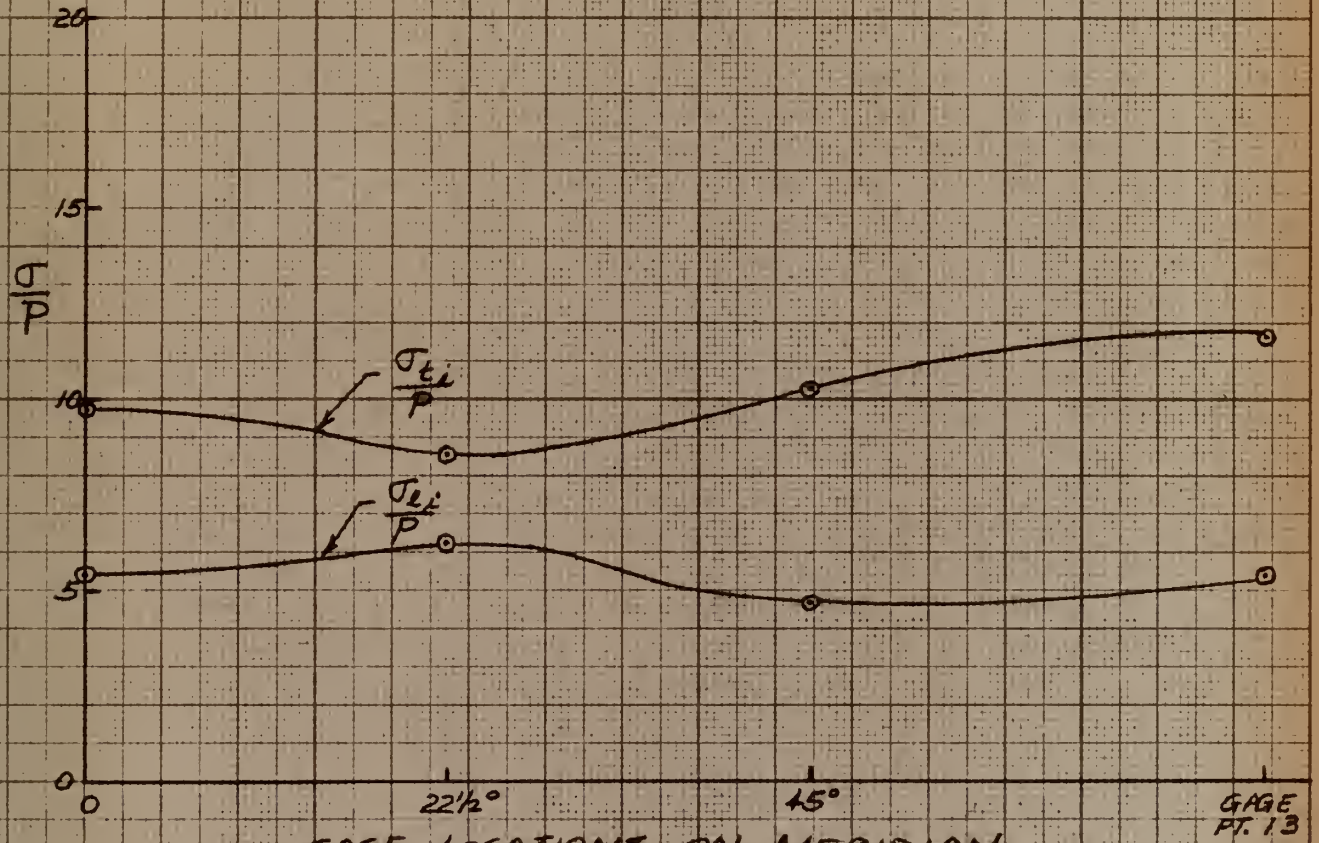

FIG. 9

SPECIMEN NO. 1

90° MERIDIAN

STRESS/PRESSURE RATIO VS. ANGULAR LOCATION

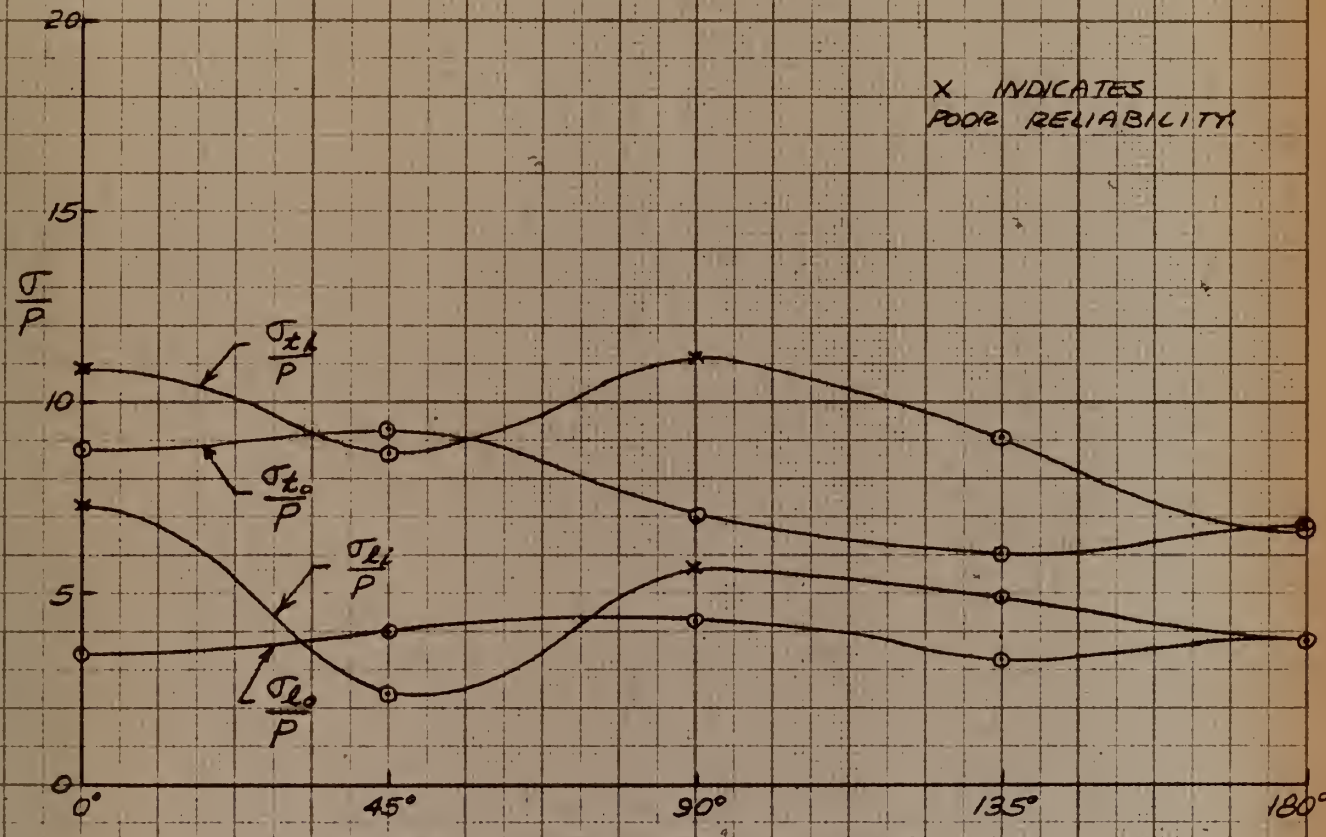

FIG. 10

SPECIMEN NO. 2

SYMMETRIC CROSS SECTION

STRESS/PRESSURE RATIO VS. ANGULAR LOCATION

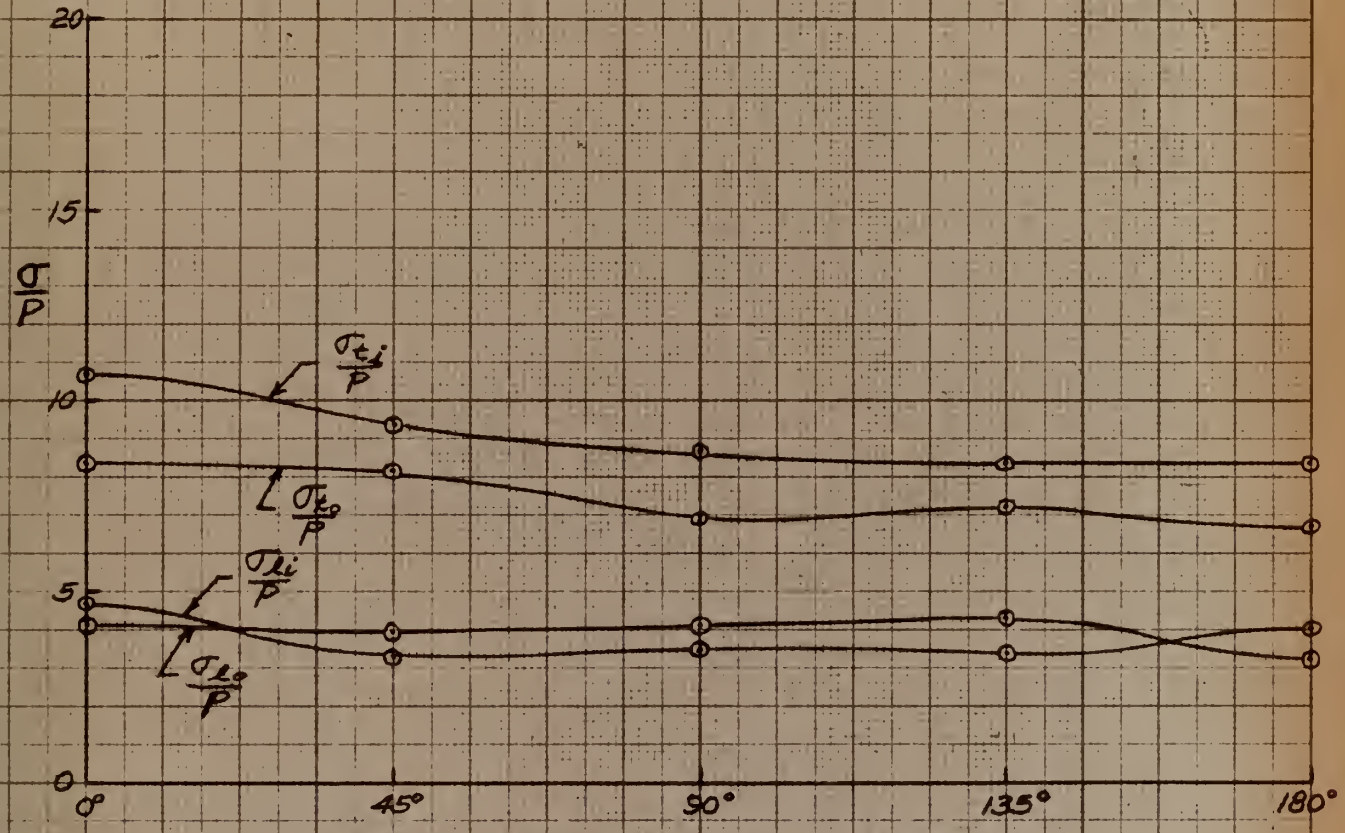

FIG. 11

SPECIMEN NO. 2

TRANSITION CROSS SECTION

STRESS/PRESSURE RATIO VS. ANGULAR LOCATION

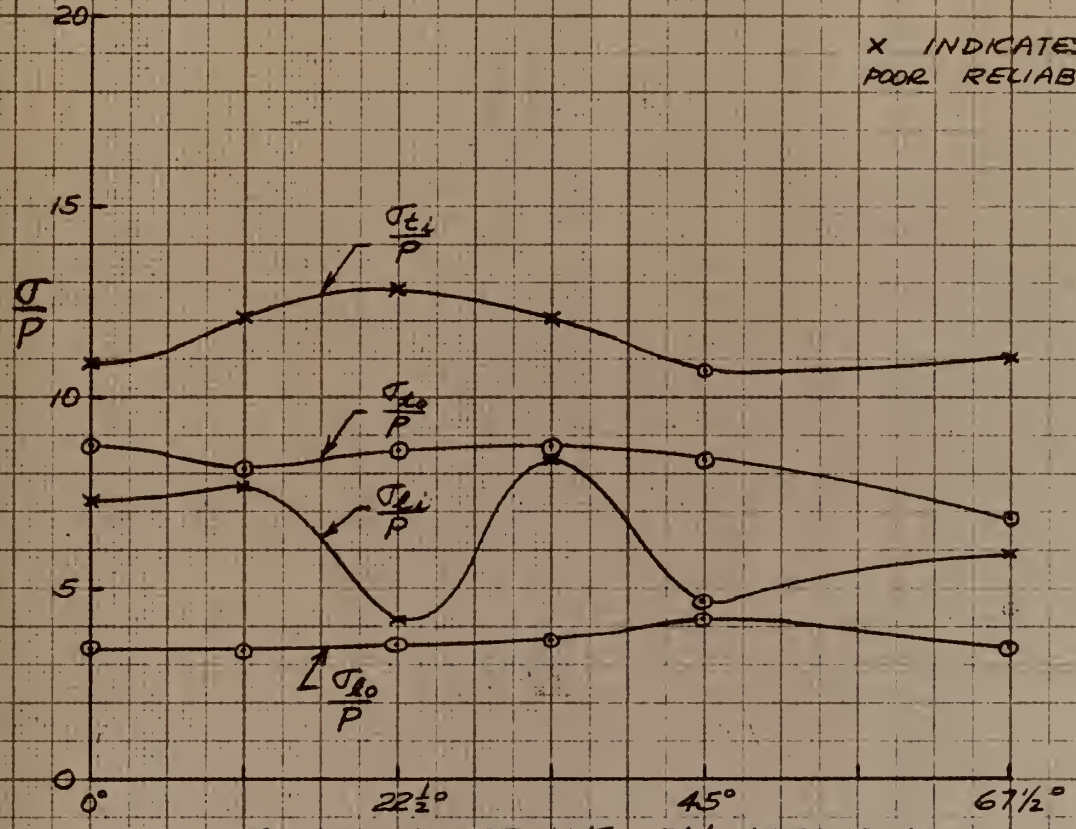

FIG. 12

SPECIMEN NO. 2

0° MERIDIAN

STRESS/PRESSURE RATIO VS. ANGULAR LOCATION

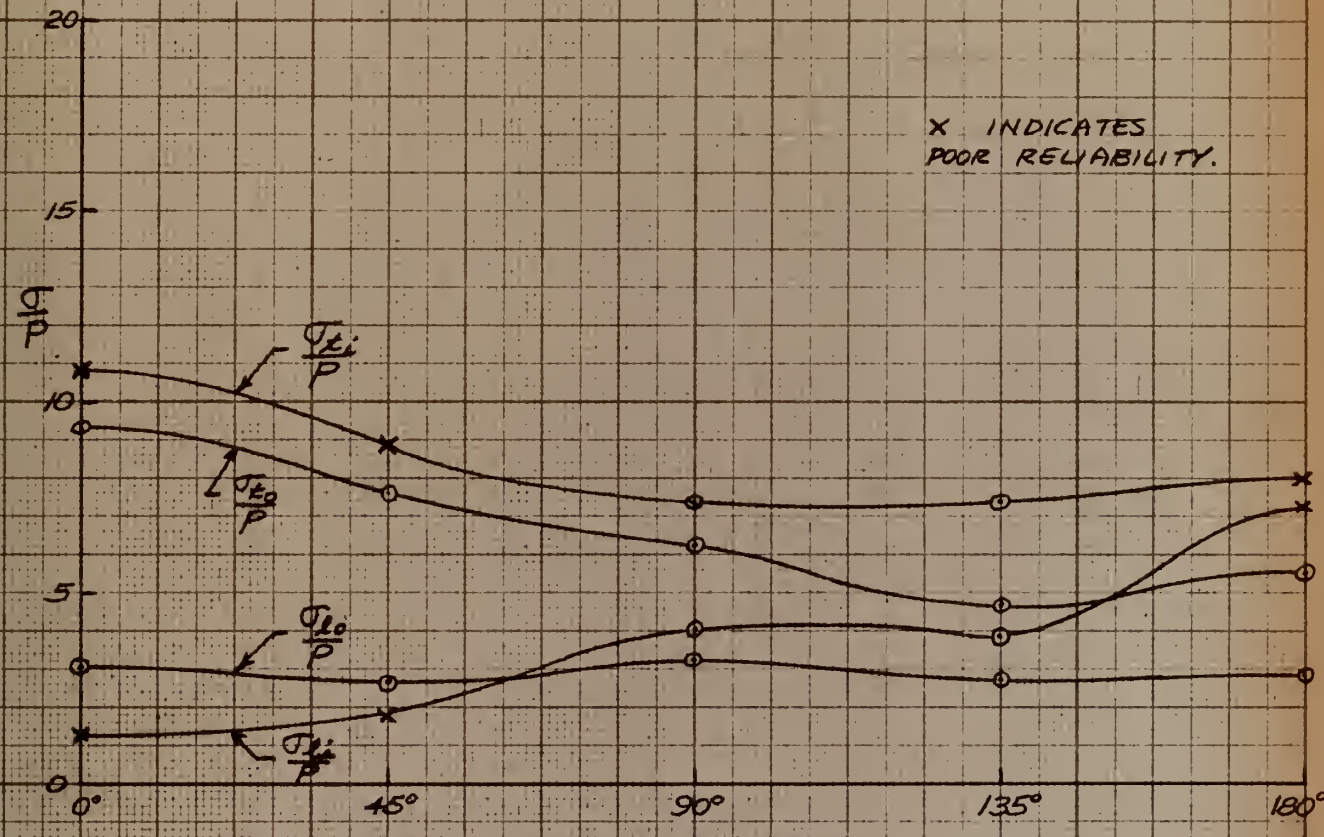

FIG. 13

SPECIMEN NO. 4

SYMMETRIC CROSS SECTION

STRESS/PRESSURE RATIO VS. ANGULAR LOCATION

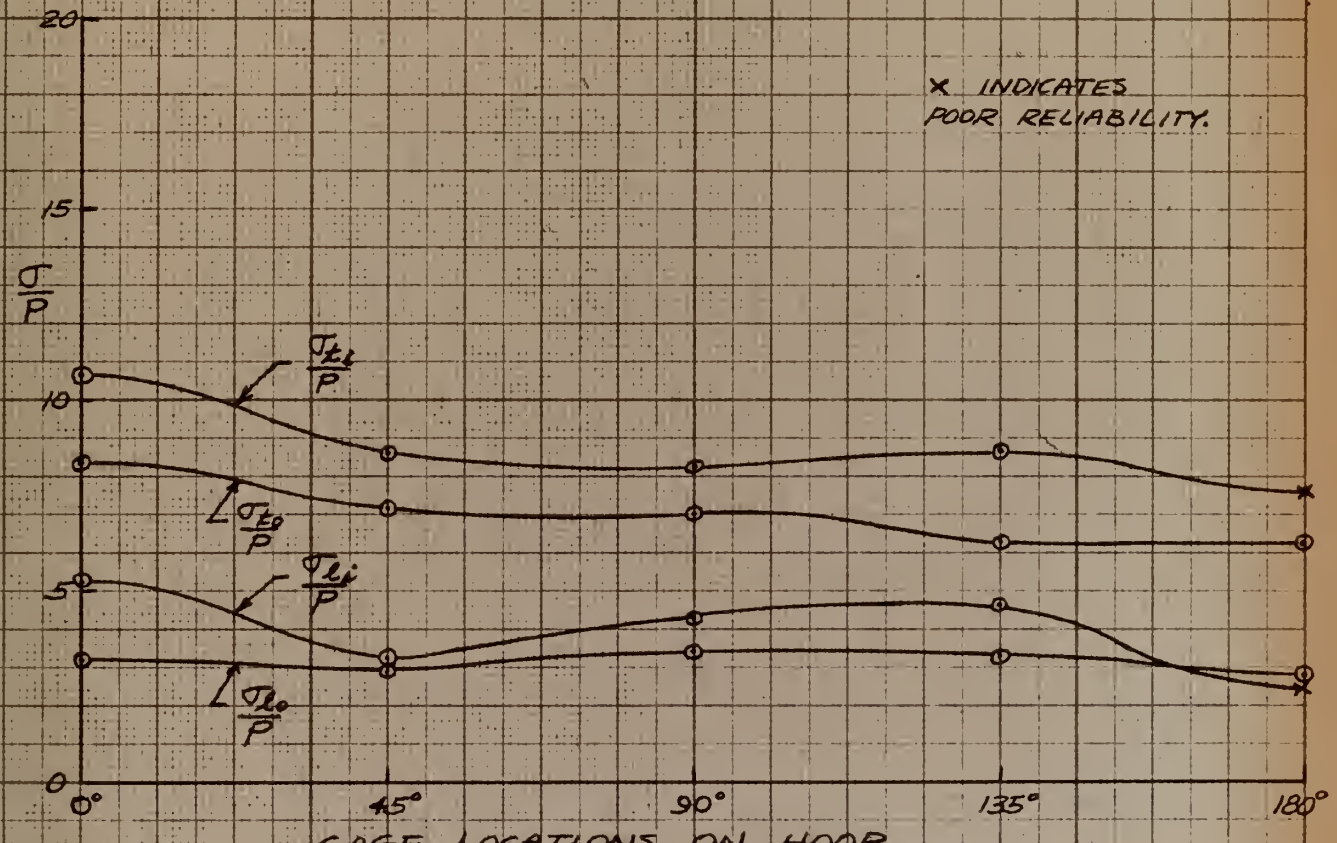

FIG. 14

SPECIMEN NO. 4

TRANSITION CROSS SECTION

STRESS/PRESSURE RATIO VS. ANGULAR LOCATION

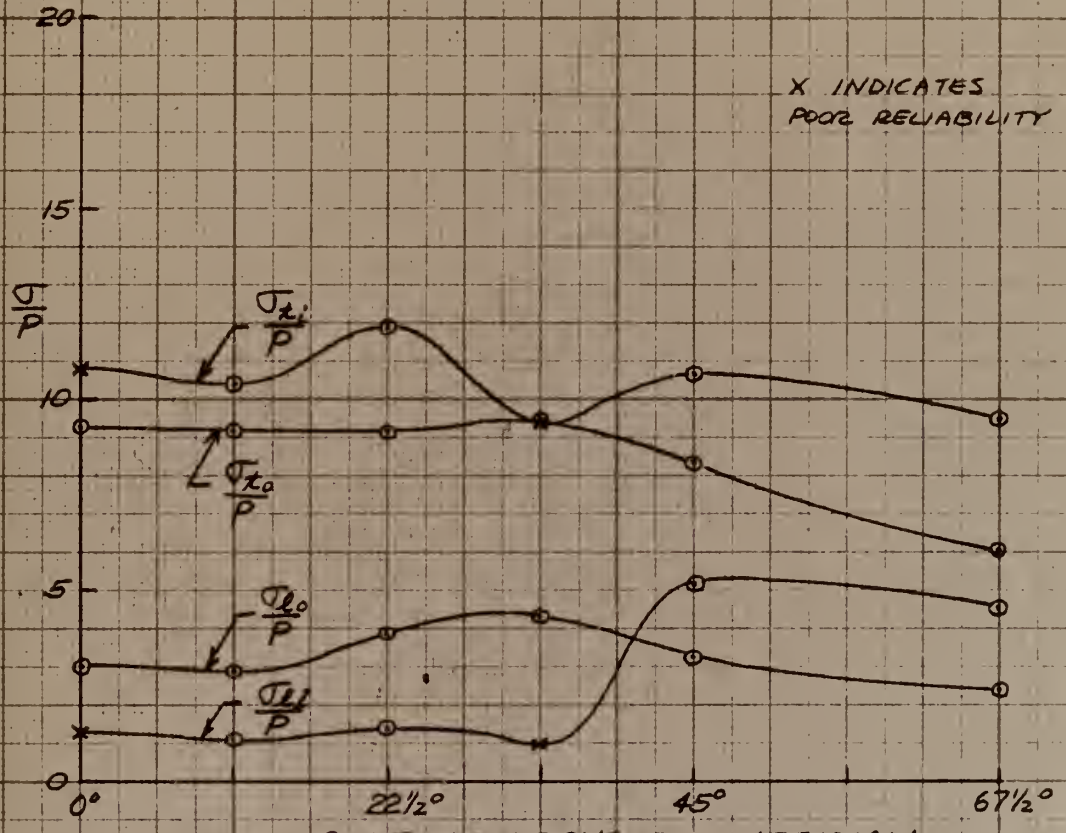

FIG. 15

SPECIMEN NO. 4

0° MERIDIAN

STRESS/PRESSURE RATIO VS. ANGULAR LOCATION

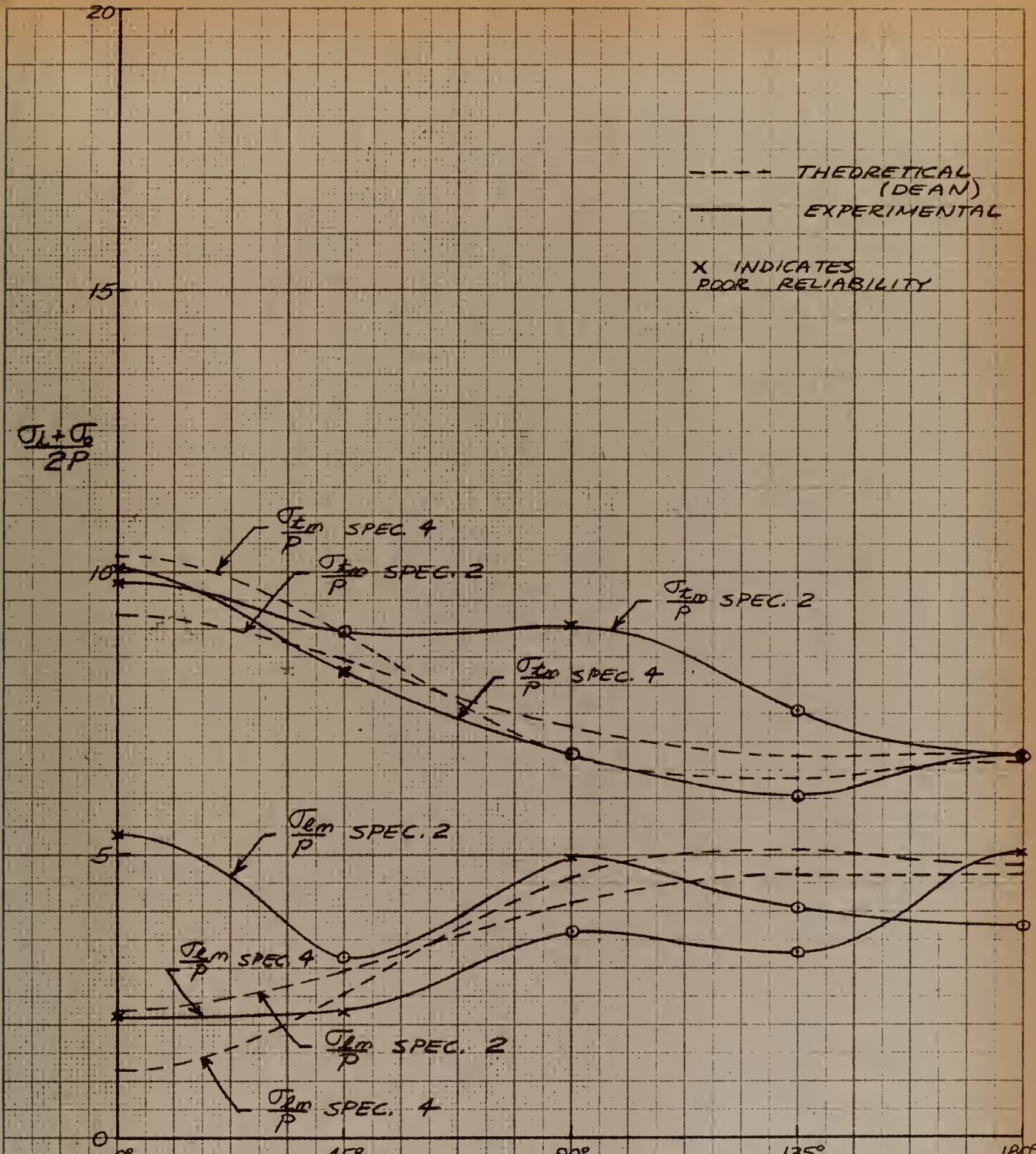

FIG. 16

SPECIMENS 2 & 4

SYMMETRIC CROSS SECTION

MEAN STRESS/PRESSURE RATIO VS. ANGULAR LOCATION

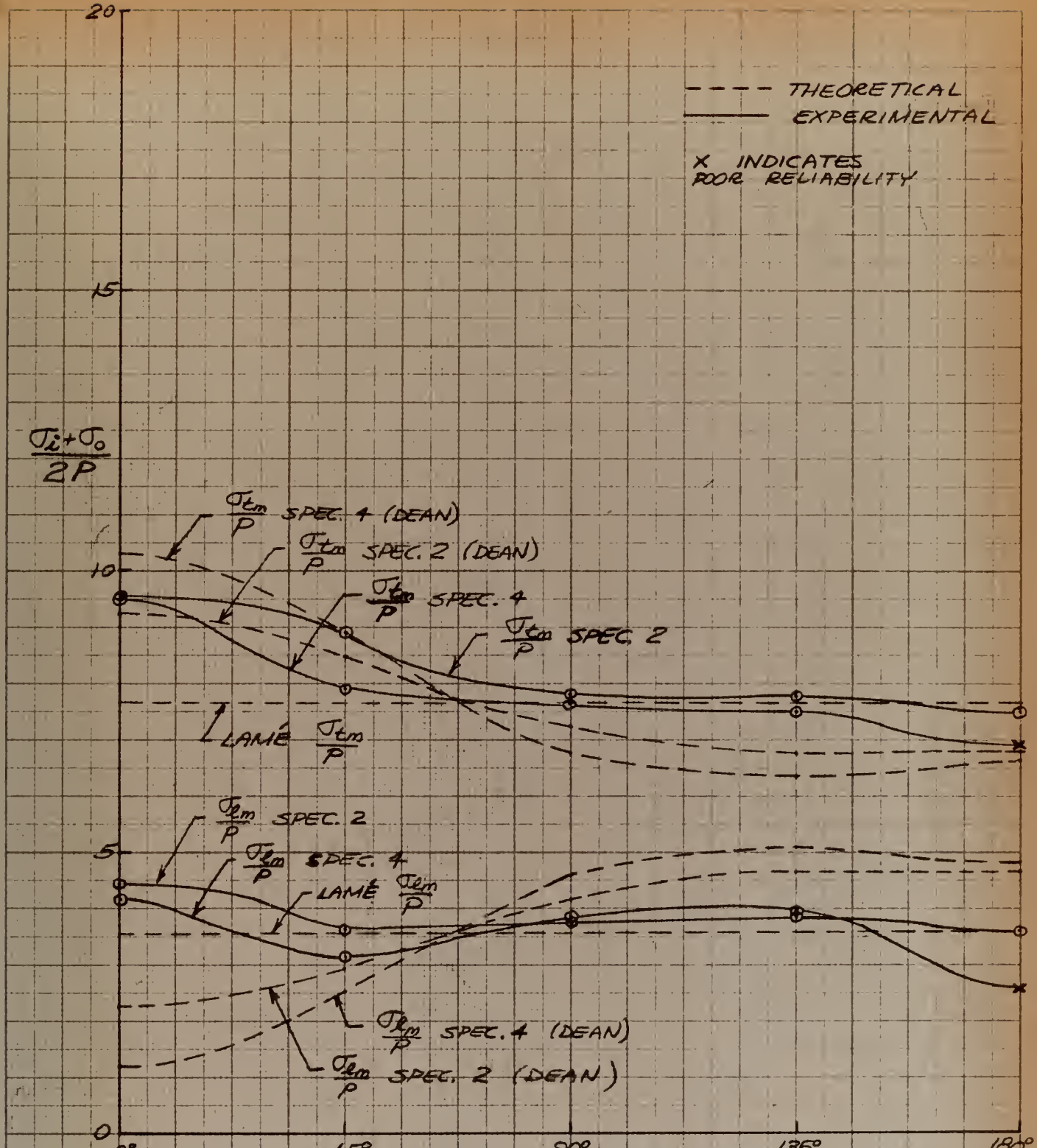

FIG. 17
SPECIMENS 2 & 4
TRANSITION CROSS SECTION
MEAN STRESS/PRESSURE RATIO VS. ANGULAR LOCATION

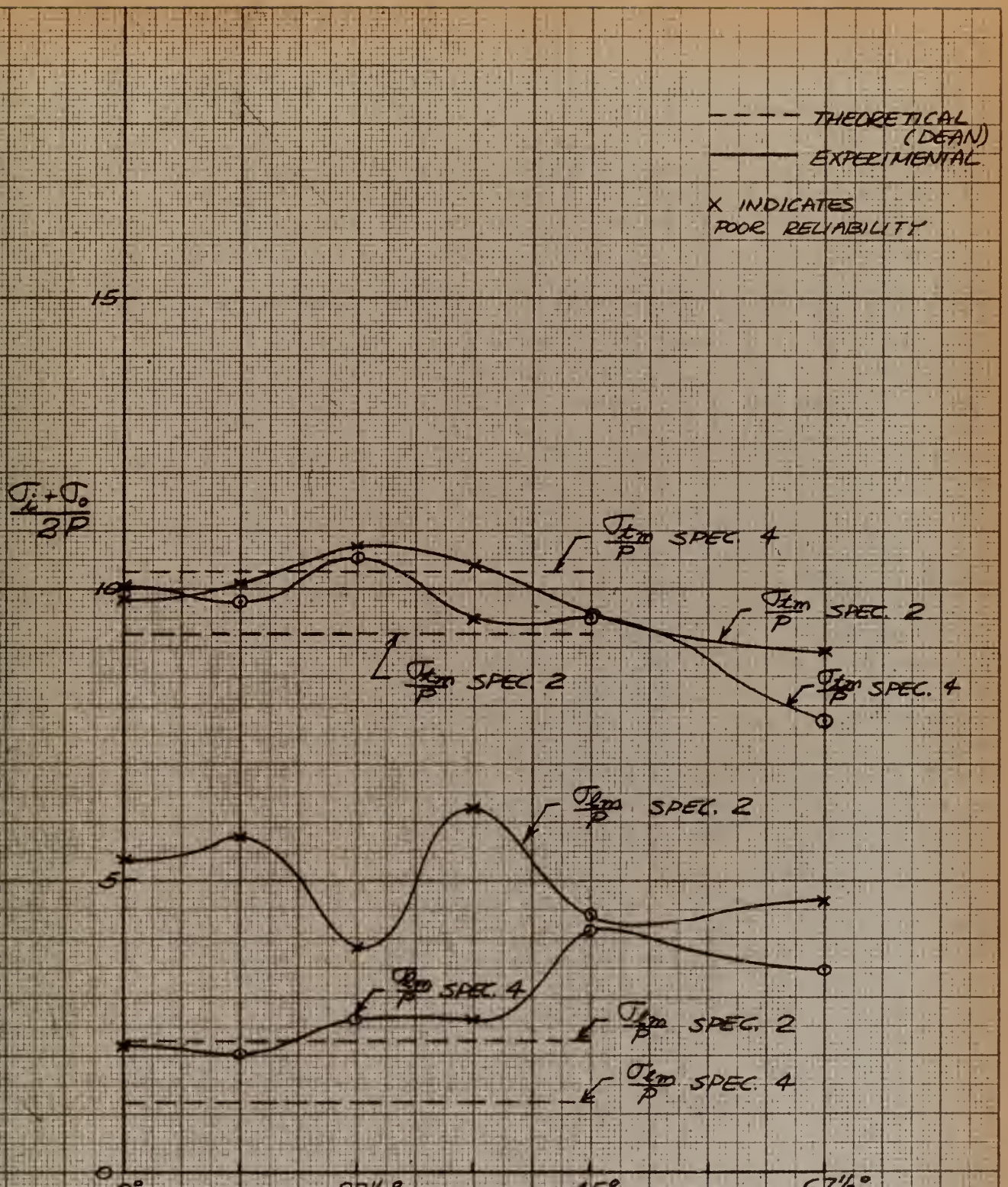

FIG. 18
SPECIMENS 2 & 4
0° MERIDIAN
MEAN STRESS/PRESSURE RATIO VS. ANGULAR LOCATION

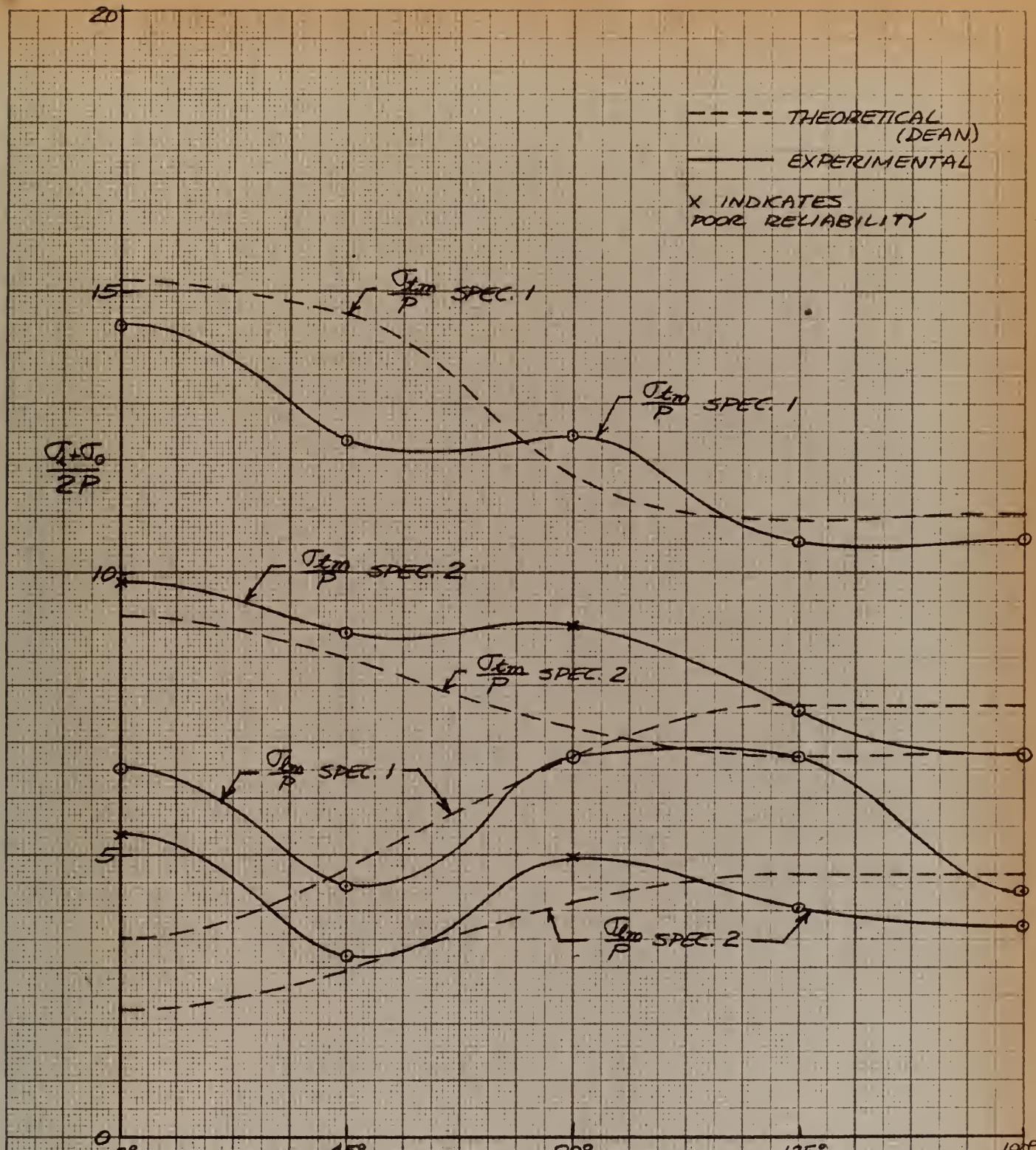

FIG. 19

SPECIMENS 1 & 2

SYMMETRIC CROSS SECTION

MEAN STRESS/PRESSURE RATIO VS. ANGULAR LOCATION

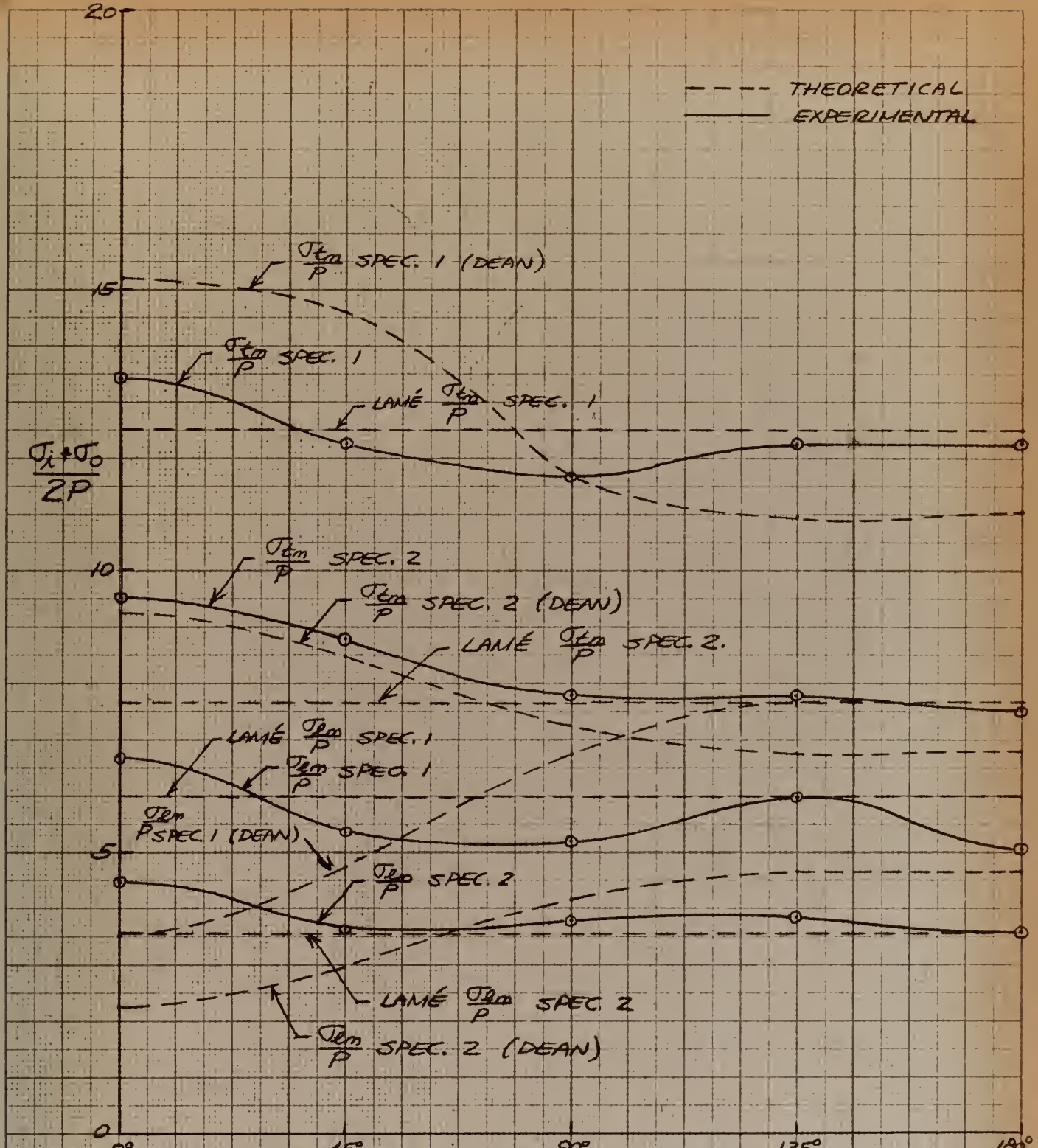

FIG. 20
SPECIMENS 1 & 2
TRANSITION CROSS SECTION
MEAN STRESS/PRESSURE RATIOS VS. ANGULAR LOCATION

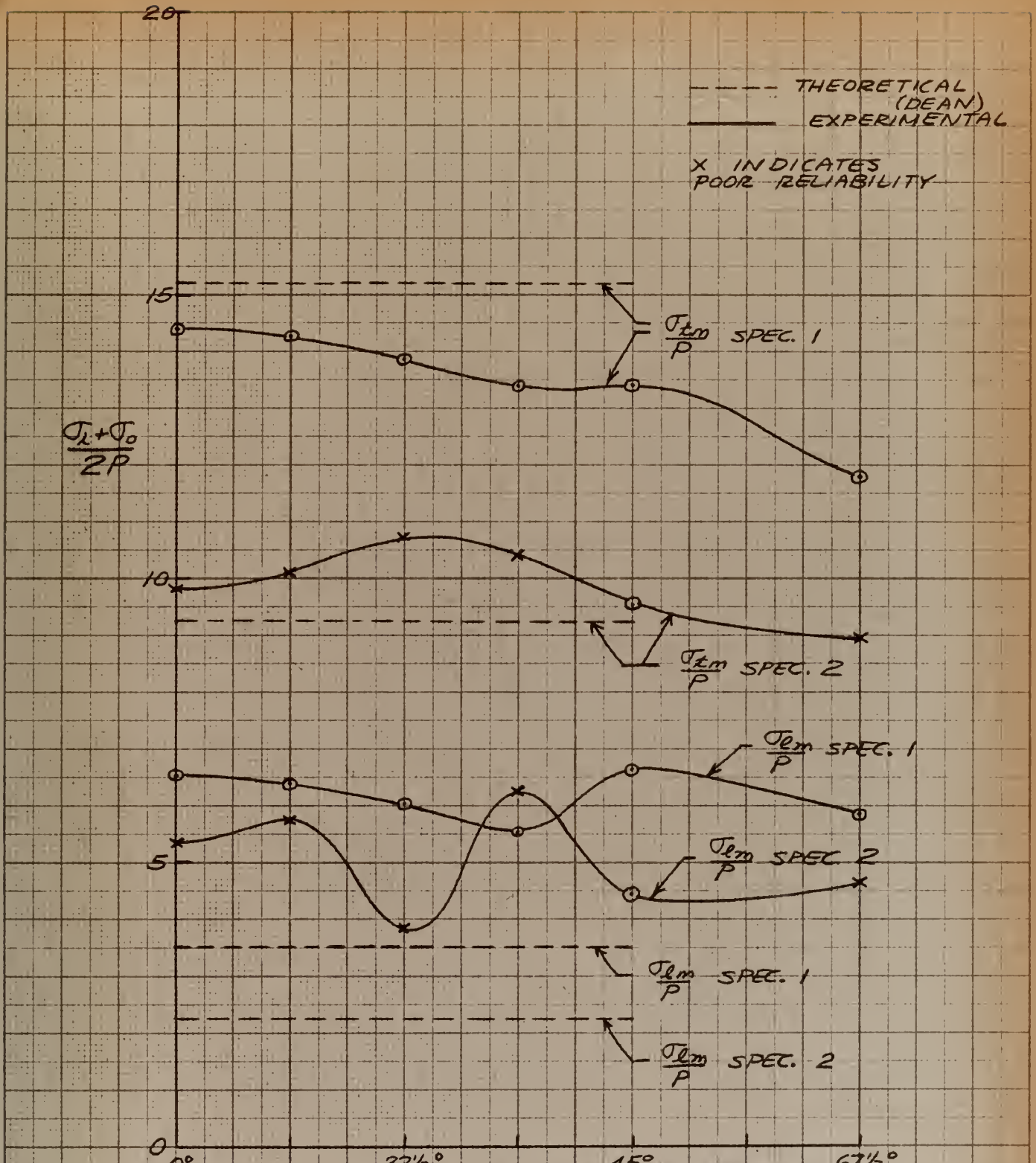

FIG. 21

SPECIMENS 1 & 2

0° MERIDIAN

MEAN STRESS/PRESSURE RATIO VS. ANGULAR LOCATION

CHAPTER V

CONCLUSIONS

The maximum stress at any cross section is found at the 0° meridian as predicted by theory and reported by L and M. The maximum stress along the 0° meridian occurs at the $22\ 1/2^{\circ}$ cross section (quarter point of the bend) in the 3 specimens tested as indicated by L and M, but differs only slightly from the values at adjacent cross sections along this meridian.

The principal stress directions remain substantially coincident with the l and t directions at the transition section where the elbow and straight end extension are joined as found by L and M.

The stress distribution in general is considerably influenced by small deviation from circularity at cross sections.

The results obtained on the external surfaces are in general in agreement with those reported by L and M with the exception of $\frac{\sigma_{te}}{P}$ values at the transition section of Specimen No. 4. Considerable deviation in many cases in the results on the internal surfaces from those of L and M is noted. This is attributed to the present use of single element gages on inside surfaces in preference to the less reliable rosette and X-types and to the fact that more time was available for improvement of specimen surfaces on which gages were cemented.

Conclusions relative to the technique of using SR-4 strain gages when subjected to pressure are contained in Appendix II.

BIBLIOGRAPHY

1. Baumberger, R., and F. Hines — Practical Reduction Formulas for use of Bonded Wire Strain Gages in Two-Dimensional Stress Fields. Society for Experimental Stress Analysis. Proceedings, Vol. II, No. 1, p. 113-127. 1945.

2. Clough, W. R., M. E. Shank, and Melvin Zaid — The Behavior of SR-4 Wire Resistance Strain Gages on Certain Materials in the Presence of Hydrostatic Pressure. Society for Experimental Stress Analysis. Proceedings. Vol. X, No. 2, p. 167-176. 1952.

3. Dean, W. R. — The Distortion of a Curved Tube due to Internal Pressure. Philosophical Magazine. Ser. 7, 28:452-464. 1939.

4. Föppl, A. — Vorlesungen über Technische Mechanik. III Festigkeitslehre. 228-229. München, Oldenbourg, 1951.

5. Kooistra, L.F. and R.U. Blaser — Experimental Technique in Pressure-Vessel Testing. ASME Transactions 72:579-587. 1950.

6. Le Ber, R. J., and J. W. Morrison — Stresses in Pipe Ells Under Internal Pressure. Thesis, U.S.N. Postgraduate School, 1953.

7. Lee, G. H. — An Introduction to Experimental Stress Analysis. New York, Wylie, 1950.

8. Timoshenko, S., and J. N. Goodier — Theory of Elasticity. New York, McGraw-Hill, 1951.

APPENDIX I

METHOD OF REDUCTION OF DATA

The stresses for the various exterior gage locations were obtained from the apparent strain data by the use of reduction formulas found in any standard text. In the case of inside gages where the block on which the compensating gage was mounted was subjected to hydrostatic pressure, and in the case of single element gages as used in these experiments, special modifications of these general methods were used.

Apparent strains were found in the units of microinches per inch per psi. This was done by plotting the raw data of apparent strain (dial reading on the Model K indicator) versus pressure and determining the slope of the best straight line through the points. Figure I-1 is a sample plot of typical gages.

For outside gages, with the compensating gage not subjected to hydrostatic pressure, the formulas for obtaining strain and stress as given by G. H. Lee [7] were used. These formulas are:

$$\epsilon_t = e_t - k e_\ell$$

$$\epsilon_\ell = e_\ell - k e_t$$

$$\sigma_t = \frac{E}{1-\nu^2}\left(\epsilon_t + \nu \epsilon_\ell\right)$$

$$\sigma_\ell = \frac{E}{1-\nu^2}\left(\epsilon_\ell + \nu \epsilon_t\right) .$$

The angle between the maximum principal stress direction and the tangential direction is given by the expression:

$$\phi = \frac{1}{2} \tan^{-1} \frac{2e_b - e_t - e_\ell}{e_t - e_\ell} .$$

For the inside gages, special note had to be taken of the fact that the block upon which the compensating gage was mounted was subjected to hydrostatic pressure. This problem is discussed at length by L. F. Kooistra and R. U. Blaser [5] and will not be taken up here. The final equation for the stresses can be found to be, for X-type gages,

$$\sigma_t = \frac{E}{1-\nu^2}\left(\bar{\epsilon}_t + \nu\bar{\epsilon}_\ell\right) - P$$

$$\sigma_\ell = \frac{E}{1-\nu^2}\left(\bar{\epsilon}_\ell + \nu\bar{\epsilon}_t\right) - P$$

where the strains are found in the usual manner, neglecting pressure effects on the compensator mounting block.

The use of single element gages required, first, the computation of a "gage factor" to be set on the Type K indicator. This factor differs from that given by the manufacturer since the gage is not subjected to a purely uniaxial stress system. R. Baumberger and F. Hines [1] give the equations needed for this computation. For the A-5 gages used in these experiments, the manufacturer's gage factor of 2.03 became 2.048 when the transverse sensitivity factor of 0.035 is given in a table in the above mentioned article was used.

When the single element gages were used, the apparent strains, and consequently the stresses, at the selected gage locations were obtained by plotting the magnitudes of the strain readings per unit of pressure versus the actual location of the various gages. Smooth curves were then drawn through the points and the apparent strains at the specified points were taken from these curves. Samples of these curves are given in Figure I-2. All available knowledge such as horizontal tangents and principal directions along planes of symmetry was

used in fairing these curves. This assisted in locating the curve properly with only a few data points. Stresses were computed at these locations in the longitudinal and tangential directions by the use of the formulas for inside X-type gages mentioned above. The only use made of the 45° (b direction) strains was in the determination of the angle between the maximum principal stress and the t direction. This was done by use of the relation

$$\phi = \frac{1}{2} \tan^{-1} \frac{2\bar{e}_b - \bar{e}_t - \bar{e}_\ell}{\bar{e}_t - \bar{e}_\ell} .$$

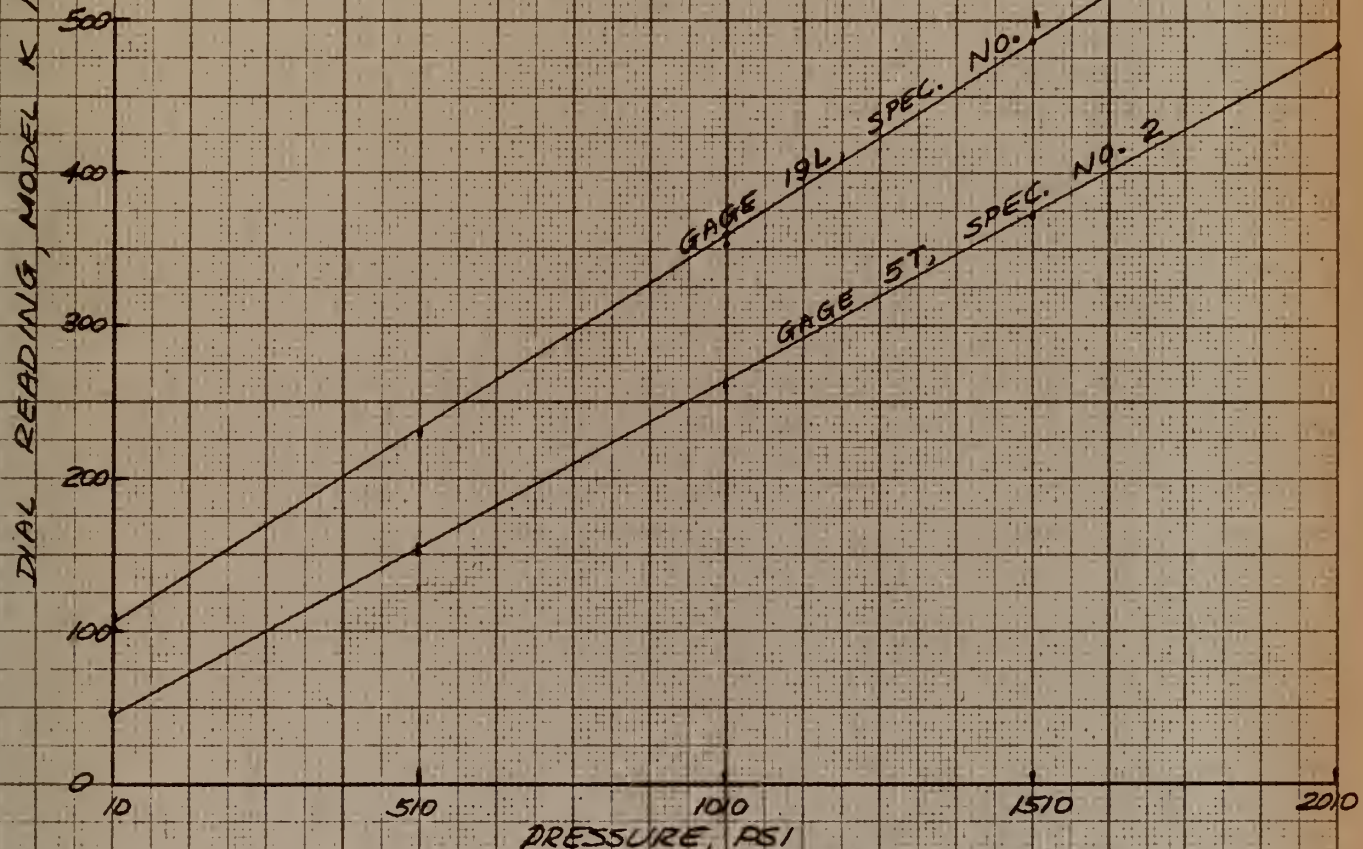

FIG. I-1.

TYPICAL CURVES SHOWING METHOD OF PLOTTING DIAL READINGS TO OBTAIN UNCORRECTED STRAIN/PRESSURE RATIOS

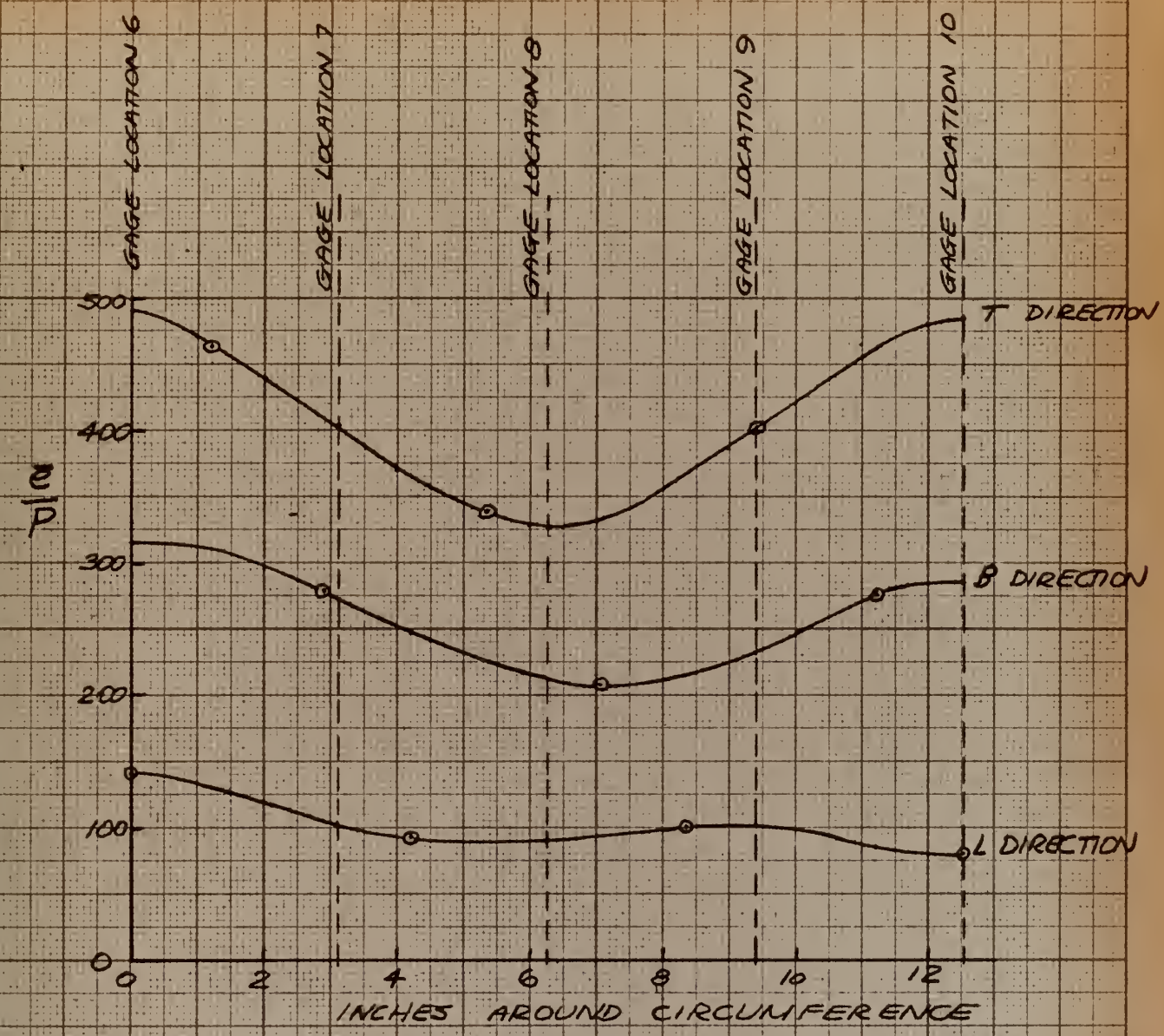

FIG. I-2.

SPECIMEN NO. 1

TRANSITION SECTION

METHOD OF OBTAINING UNCORRECTED APPARENT STRAIN FOR VARIOUS LOCATIONS

(⊙ DENOTES ACTUAL GAGE.)

APPENDIX II

BEHAVIOR OF SR-4 STRAIN GAGES UNDER STATIC PRESSURE

Considerable difficulty in obtaining reliable data from internal strain gages subjected to pressure was experienced in the tests of Specimens 2 and 4. Some difficulty of this nature was expected in view of statements by L and M and the work of W. R. Clough, M. E. Shank and M. Zaid [2].

Le Ber and Morrison reported very poor reliability in numerous instances with AR-1 type gages and in several instances with AX-5 type gages. Clough, Shank and Zaid conducted a number of experiments with SR-4 type A-14 strain gages under pressure. They studied the case of two identical gages placed in different arms of a Wheatstone bridge so as to theoretically give a null reading. In no instance was a null reading actually obtained but variations from the null as large as 25 microinches per inch per 1000 psi pressure were read.

In view of expected difficulties several preliminary tests were conducted with A-5 and A-7 type single element gages to determine which was the better type for use as replacements for the unreliable internal rosette gages already installed in the test specimens. The grid of the A-5 gage is manufactured flat and in one plane while that of the A-7 is wound about a cylinder and then pressed flat so that its grid wire is not coplanar. Several A-5 and A-7 gages were installed on the internal surface in the straight pipe portion of Specimen 2 in the tangential direction. Additional gages of the same types were mounted on two small metal blocks, one of which was flat and the other curved to the

same radius as that of pipe. These blocks were placed inside the pipe.

Strain readings were taken with the tangential active gages using first the flat and then the curved mounted gage as compensator. Also readings were taken with the flat mounted and curved mounted gages connected to the strain indicator in such a way as to give a theoretical null reading. Maximum pressure of 2000 psi was used in these tests.

The results of these preliminary tests indicated the superiority of the A-5 over the A-7 type for the intended application. A null reading was in fact obtained, over the pressure range used, when the flat mounted A-5 and the A-5 mounted on the curved block were both in the bridge circuit. Also essentially duplicate readings of tangential A-5 gages were obtained using either of the block mounted gages as compensators. Further, these readings were in good agreement with theory for straight pipe.

With the A-7 gages, readings of the order of -20 microinches per inch were obtained at 2000 psi where a null reading was theoretically expected. This behavior with A-7 gages was similar in nature to that reported by Clough, Shank and Zaid for A-14 gages.

During the course of subsequent experimentation with the three pipe specimens A-5 gages consistently gave reliable results in every case. Internal compensators were frequently checked under pressure with an external temperature compensating gage to insure their behavior remained constant and reliable.

Approximately 50% of the AX-5 gages which had previously been installed by L and M or which were replaced by the authors in Specimens

2 and 4 exhibited some degree of unreliability. Figure II-1 contains typical curves of data obtained with unreliable AX-5 gages.

The behavior referred to by L and M as "zero drift" was encountered. It was observed, however, in numerous instances that if sufficient time were allowed after a pressure cycle the gage reading would return to its initial value. The time required for this return varied from several minutes for some gages to more than an hour for others. Figure II-2 is a plot of variation in the indicated strain of one gage element with time at a pressure of 1510 psi.

The variation in indicated strain reading with time at constant pressure was, for essentially all gages which exhibited unreliable characteristics, a greater extensional strain if pressure had immediately before been increased and a lesser extensional strain if pressure had just been reduced. This behavior resulted in algebraically higher readings at a given pressure in the descending portion of a pressure cycle from 2000 to 0 psi than in the ascending portion.

In the authors' opinion the unusual behavior of AX-5 gages under pressure was due to the presence of small indentations in the surface on which the gage was mounted or air bubbles in the cement, or both. It is believed that the cement exhibited creep under pressure when such inhomogeneities were present in the cement. It is believed that as pressure was increased on these strain gages the grid wire was distorted and forced into indentations in the surface of the pipe or into air bubble voids in the cement, thereby increasing its reading. The variation of

this reading with time is believed to be due to creep of the cement permitting the deformation of the gage grid wire to increase with time with increasing pressure and to eventually return to its initial configuration after pressure was released. The "memory effect" of many plastics is a well known phenomenon.

On the basis of the authors' experience the following conclusions and recommendations are made relative to the use of SR-4 strain gages when subjected to pressure:

(a) Single element flat grid A-5 strain gages can be made to give reliable results under pressure. For this service they are superior to X-type, 3 element rosette type, and single element wound type gages.

(b) Surfaces on which gages are to be cemented should be prepared with greater than usual care, eliminating even slight indentations and pits into which pressure could force the grid wire.

(c) Careful attention to uniform cement thickness, minimum number of air bubbles, and the allowance of double the standard drying time are considered important for gages subjected to pressure.

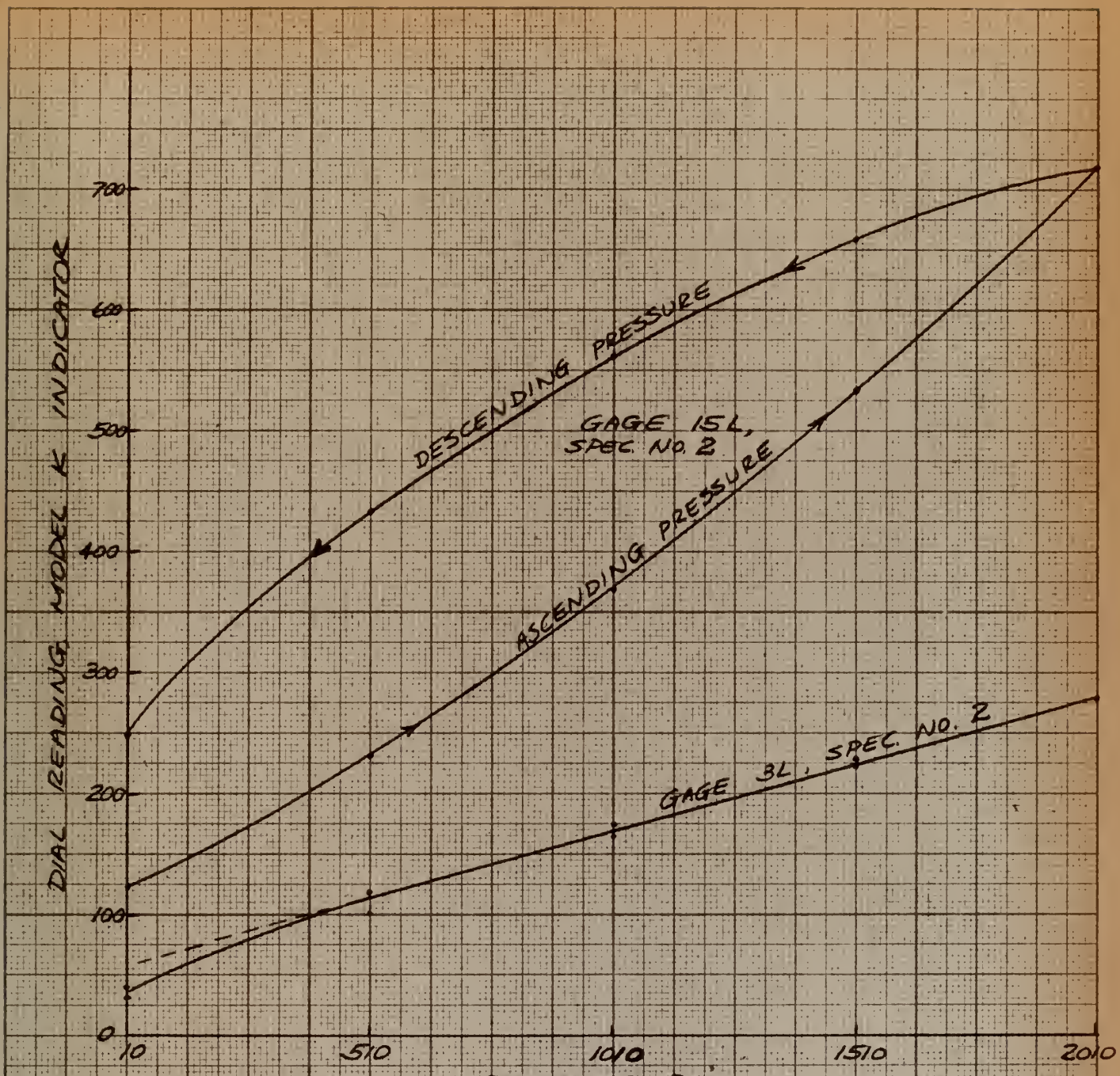

FIG II-1

DIAL READING VS. PRESSURE
FOR VARIOUS INSIDE GAGES
SHOWING EXTREMES OF
MISBEHAVIOR ENCOUNTERED

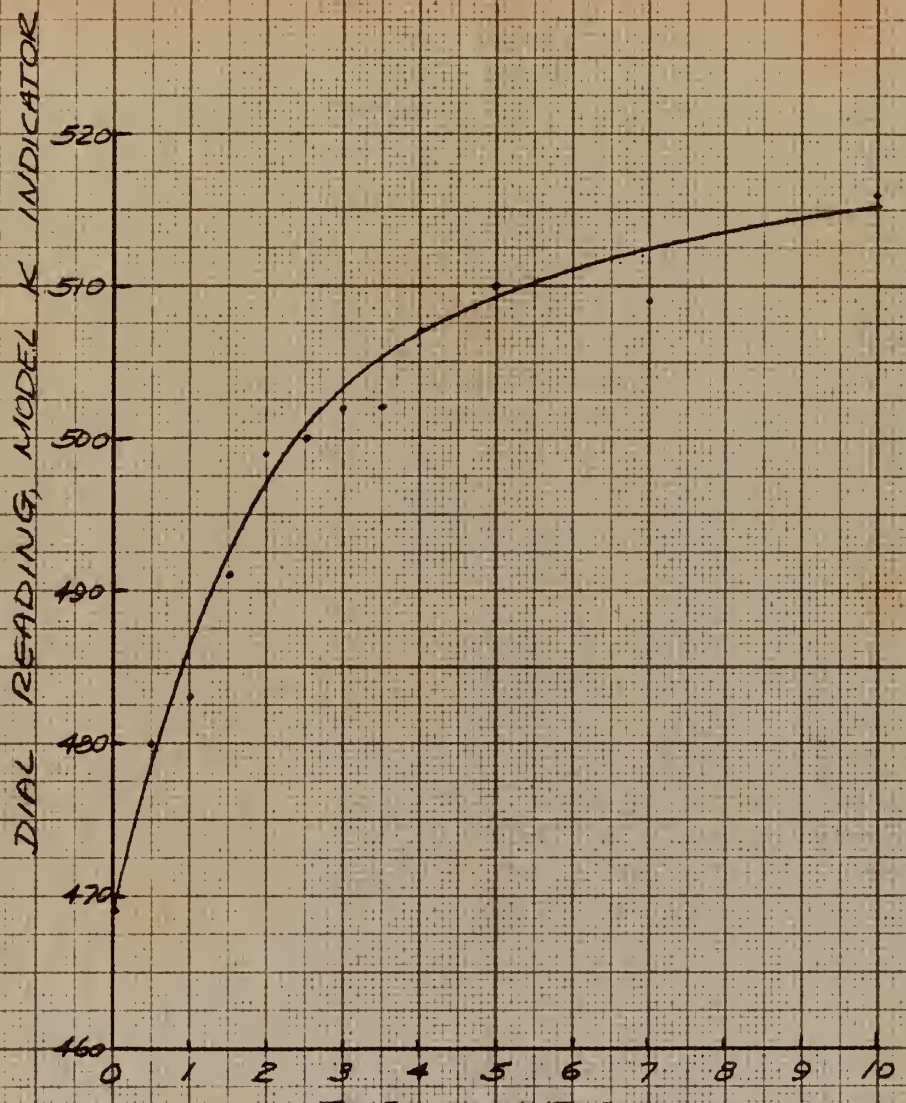

FIG. II-2
SPECIMEN NO. 2

VARIATION OF DIAL READING WITH TIME FOR FIXED PRESSURE, 1510 PSI
GAGE NO. 15L

APPENDIX III

THEORETICAL FORMULAE

1. Lamé solution for thick walled straight pipe under internal hydrostatic pressure

$$\frac{\sigma_t}{P} = \frac{r_i^2}{r_o^2 - r_i^2}\left(1 + \frac{r_o^2}{r^2}\right)$$

$$\frac{\sigma_l}{P} = \frac{r_i^2}{r_o^2 - r_i^2} \quad \text{from equilibrium considerations.}$$

2. Föppl solution (membrane analysis of torus under internal pressure)

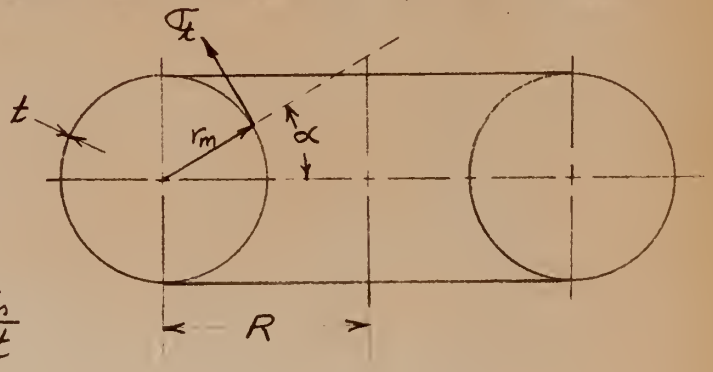

$$\frac{\sigma_t}{P} = \frac{2R - r_m \cos\alpha}{R - r_m \cos\alpha} \cdot \frac{r_m}{2t}$$

$$\frac{\sigma_l}{P} = \frac{r_m}{2t}$$

3. Dean solution for torus under internal pressure

$$\frac{\sigma_t}{P} = \frac{r_i}{t}\left[1 + \frac{r_i \cos\alpha}{2R} + \frac{r_i^2 \cos 2\alpha}{2R^2}\right]$$

$$\frac{\sigma_l}{P} = \frac{r_i}{2t}\left[1 - \frac{r_i \cos\alpha}{R} - \left(1 - \frac{\nu}{4}\right)\frac{r_i^2 \cos 2\alpha}{R^2}\right].$$

25270
Thesis Price
P943 Stress distribution in pipe ells with straight end extensions under internal pressure.